

Spikes in Poissonian quantum trajectories

Alan Sherry,^{1,*} Cedric Bernardin,^{2,†} Abhishek Dhar,^{1,‡} Aritra Kundu,^{3,§} and Raphael Chetrite^{4,¶}

¹*International Centre for Theoretical Sciences, Tata Institute of Fundamental Research, Bangalore 560089, India*

²*Faculty of Mathematics, National Research University Higher School of Economics, 6 Usacheva, Moscow, 119048, Russia.*

³*Department of Physics and Materials Science, University of Luxembourg, L-1511 Luxembourg*

⁴*Institut de Physique de Nice (INPHYNI), Université Côte d'Azur, CNRS, 17 rue Julien Lauprêtre, Nice, 06200, France*

We consider the dynamics of a continuously monitored qubit in the limit of strong measurement rate where the quantum trajectory is described by a stochastic master equation with Poisson noise. Such limits are expected to give rise to quantum jumps between the pointer states associated with the non-demolition measurement. A surprising discovery in earlier work [Tilloy *et al.*, Phys. Rev. A **92**, 052111 (2015)] on quantum trajectories with Brownian noise was the phenomena of spikes observed in between the quantum jumps. Here, we show that spikes are observed also for Poisson noise. We consider three cases where the non-demolition is broken by adding, to the basic strong measurement dynamics, either unitary evolution or thermal noise or additional measurements. We present a complete analysis of the spike and jump statistics for all three cases using the fact that the dynamics effectively corresponds to that of stochastic resetting. We provide numerical results to support our analytic results.

CONTENTS

I. Introduction	2	A. Example 1 with resetting: Non-Quantum SDEs	13
II. General setup: stochastic master equation (SME) of d -dimensional systems with Poisson noise	2	B. Example 2 without resetting: Collapse-Thermal setup with general QND (diagonal) measurement N_1 operator	14
A. Large time limit of the SME Eq. (1): to collapse or not	3	C. Example 3 with resetting: Collapse-Measurement setup for QND resetting $N_1 = - \rangle \langle - $ but general N_2 operator	15
B. Strong collapse Zeno limit in a non-QND setup: Quantum jump phenomenon versus Spikes phenomenon	3	VII. Conclusion	16
III. Precise setup: SME of Qubit for Non-Demolition “reset” continuous measurement of $ - \rangle \langle - $	4	Acknowledgments	16
A. Collapse-Unitary setup: Measurement of Rabi qubit coherent oscillations	4	References	17
B. Collapse-Thermal setup: Measurement of thermal fluctuations	5	A. Measurement part of the SME Eq. (1) for qubit with a general diagonal measurement operator	19
C. Collapse-Measurement setup: Competition between two measurements	5	1. Resetting dynamics or not	19
IV. Summary of main results in the Precise setup	7	2. Proof of Eq. (A3)	20
V. Mathematical Derivations	8	B. Proof of Eq. (72) and of Eq. (23)	20
A. Study in the Collapse-Unitary setup	8	C. Proof of Eq. (17)	20
B. Study in the Collapse-Thermal setup	11	1. Proof of Eq. (C1)	21
C. Study in the Collapse-Measurement setup	12	D. Convergence of spiking process for the scaling $k_\gamma \sim \gamma^\alpha$	21
VI. Generalization: a general perspective on spikes in 1D piecewise deterministic Markov process	13	E. Exact computation and asymptotics of Laplace transforms	21
		1. Collapse-Unitary setup	21
		2. Collapse-Thermal setup	21
		3. Collapse-Measurement setup	22
		F. Numerical Methods	23

* alan.sherry@icts.res.in

† sedric.bernardin@gmail.com

‡ abhishek.dhar@icts.res.in

§ aritra.kundu@uni.lu

¶ raphael.chetrite@univ-cotedazur.fr

I. INTRODUCTION

In the last decade, the flourishing interest in feedback control of quantum systems has led to a renaissance of the theory of quantum measurements through continuous measurements. The cornerstone of continuous quantum measurements is the stochastic master equation (SME), also called the quantum trajectories equation, or the Belavkin-Barchielli equation. After an initial period of development in the spontaneous collapse community [1–4], SME was really born in the eighties in quantum optics and quantum filtering communities [5–18]. They are now part of standard textbooks [19–24], and have been observed experimentally [25–30]. In the context of the so-called Quantum Non-Demolition (QND) setup it is assumed that measurement operators, and possible Hamiltonians, are all diagonalisable in the same orthonormal basis, called the pointer basis. One of the most striking results in this case is that the large time-limiting form of the density matrix is in accordance with the usual Born rule. This has been observed experimentally [25–27] and proven theoretically in [31–35].

An interesting situation arises when one considers the non-QND setup (see Sec. II), where a lot of attention has recently been given to the case of large rate measurement limit, which is also called the strong collapse limit (or weak non-QND limit) of non-QND quantum trajectories. We then expect to see the emergence of quantum jumps between pointer states and this has been observed experimentally [36–38]. It was recently theoretically explained in [39] for SME with Gaussian noise in the Collapse-Thermal and Collapse-Unitary setups. [40] generalised [39] for SME with Gaussian noise, in more general setups, particularly the Collapse-Measurement case. [41] also discusses it for SME with Poisson noise in the Collapse-Unitary setup. Note that the quantum Zeno effect [42–47] argues that continuously observing a quantum state leads to a zero probability of evolving away from a given state, thus freezing the evolution of the system and suppressing the quantum jumps. However, the Zeno effect can be avoided if one considers the appropriate limit of system probe interactions.

A surprising discovery [48] was the observation of sharp scale-invariant fluctuations that invariably decorate the jump process (see Fig. 1c, 2c and 3c), in the limit where the measurement rate is very large. These seemingly instantaneous excursions have been referred to as *quantum spikes*. These fluctuations around the dominant jump process seem to be visible in the early numerical work on the subject [49, 50] while their first analytical description was done recently by Bauer-Bernard-Tilloy [48, 51, 52], which motivated some other works [53, 54]. Previous work has been exclusively concerned with Gaussian noise SMEs and explains these phenomena by relating it to the fact that the convergence to the jump process between pointer states is weak. However, this is expected to be valid for more general SMEs and we quote Tilloy [55]: “A first possible generalization is to go from a continuous

collapse model to a discrete one, and replace the diffusive equations we had with jump ones.....However, while spikes are numerically present as well in this context and seem to have the exact same power law statistics, no proof is known even for the qubit case.” The main goal of the current paper is to demonstrate the phenomena of quantum spikes for the case of Poisson noise SMEs and to study their statistical properties.

We limit our analytical study to particular cases of a qubit system, for the three setups which we refer to as the Collapse-Unitary setup, the Collapse-Thermal setup, and the Collapse-Measurement setup. The restriction of our study, apart from the fact that it concerns only a qubit, is that its analytical resolution is based on the fact that the resulting dynamics is in fact a 1-dimensional piecewise resetting Markov dynamics [56–59], and explicit Laplace transforms lead to the complete statistics of the associated quantum spikes. In Sec. VI we discuss our results in the context of more general piecewise deterministic Markov processes.

The plan of the paper is as follows: in Sec. II, we discuss the general set-up and then in Sec. III, explain the three specific models that we study here. In Sec. IV, we summarize the main results and present comparisons of various analytic expressions with numerical data. The mathematical derivations are presented in Sec. V. In Sec. VI, we enlarge our discussion for more abstract mathematical models and state a conjecture about the spikes statistics for the latter. We conclude the paper with a conclusion section, see Sec. VII, where we also discuss the relevance of spikes in real experimental studies.

II. GENERAL SETUP: STOCHASTIC MASTER EQUATION (SME) OF d -DIMENSIONAL SYSTEMS WITH POISSON NOISE

We consider here SMEs with Poisson white noise (discarding the possible Gaussian part of the noise), in finite d -dimensional Hilbert space, describing the real-time evolution of a quantum system with (Hermitian) density matrix ρ ($\rho \geq 0, \text{Tr}(\rho) = 1$) with free evolution given by a Hermitian Hamiltonian H , thermal evolution given by a Lindbladian L^{th} [60, 61], and simultaneous independent continuous measurement of p operators $\{N_k \in \mathcal{M}_d(\mathbb{C})\}_{k=1, \dots, p}$, where $\mathcal{M}_d(\mathbb{C})$ denotes the set of square complex matrices of size d , and with with rate of measurement $\gamma = \{\gamma_k\}_{k=1, \dots, p}$. The evolution equation of the density matrix is given by the piecewise deterministic Markov process (see for example relations (6.224-6.227) of [22])

$$\begin{aligned} \dot{\rho}_t^\gamma = & -i[H, \rho_t^\gamma] + L^{th}[\rho_t^\gamma] \\ & + \sum_{k=1}^p \left\{ \gamma_k L_{N_k}[\rho_t^\gamma] + M_{N_k}[\rho_t^\gamma] \left[\dot{\mathcal{N}}_t^{k, \gamma} - \mathbb{E} \left(\dot{\mathcal{N}}_t^{k, \gamma} | \rho_t^\gamma \right) \right] \right\} . \end{aligned} \quad (1)$$

In the previous equation:

- * The (classical) *signal measurements* $\{\mathcal{N}_t^{k,\gamma}\}_{k=1,\dots,p}$ are given by non-autonomous Poissonian processes ($d\mathcal{N}_t^{k,\gamma} \in \{0,1\}$ and $d\mathcal{N}_t^{k,\gamma} d\mathcal{N}_t^{\ell,\gamma} = d\mathcal{N}_t^{k,\gamma} \delta_{k\ell}$), with statistics

$$\mathbb{E} \left(d\mathcal{N}_t^{k,\gamma} |\rho_t^\gamma \right) = \gamma_k \eta_k \text{Tr} \left(N_k \rho_t^\gamma N_k^\dagger \right) dt. \quad (2)$$

We will refer to the signals $d\mathcal{N}_t^{k,\gamma} = 1$ as "clicks". Note that, in all the terms, ρ_t^γ in the previous equations must be understood as the density matrix taken just before an eventual jump happening at time t .

- * The *measurement operators* N_k are arbitrary matrices (not necessarily commuting, not necessarily Hermitian) and characterise each independent detector. The parameters $\eta_k \in [0,1]$ are the associated detector efficiencies: $\eta_k = 1$ (resp. $\eta_k = 0$) corresponds to a perfect efficient detector (resp. an unread measurement).
- * The *Lindbladian* [62] operator L_N , associated to the measurement operator N , encapsulates the back-effect of the N -measurement on the average evolution. It is given by [60, 61]

$$L_N [\rho] = N \rho N^\dagger - \frac{1}{2} N^\dagger N \rho - \frac{1}{2} \rho N^\dagger N. \quad (3)$$

- * The *stochastic innovation* $M_N [\rho]$ is the non-linear operator defined by

$$M_N [\rho] = \frac{N \rho N^\dagger}{\text{Tr}(N \rho N^\dagger)} - \rho. \quad (4)$$

From a theoretical viewpoint, the simplest way to derive the SME Eq. (1) from ideal physical systems is as the limit of infinitely strong and frequent indirect measurements, see for example [22, 24, 63]. The non-linearity in Eq. (1) is a remnant of the non-linear updating of all type of Bayesian measurements. However, this non-linearity is in fact the effect of the fixed normalisation $\text{Tr}(\rho_t^\gamma) = 1$, since, without this normalisation, Eq. (1) can be formulated as a linear equation [19–24].

Note that in practice, for a real experiment, the knowledge about the quantum system is only stored in the Poisson signal process $\{\mathcal{N}_t^{k,\gamma}\}_{k \in 1,\dots,p}$. The density matrix ρ_t^γ itself, is not directly observable, and is only reconstructed from the Poisson signal process.

A. Large time limit of the SME Eq. (1): to collapse or not

The first crucial question concerning the SME Eq. (1) is the understanding of its large-time behaviour. Let us assume for the moment that we do not have any thermal bath $L^{th} = 0$. The *Quantum Non-Demolition*

(QND) hypothesis [20, 21, 25, 64–69] is the fact that there exists an orthonormal basis $\{|e_i\rangle\}_{i=1,\dots,d}$, called the *pointer basis* [70], such that all the measurement operators $\{N_k\}_{k=1,\dots,p}$, and the Hamiltonian H , are diagonal in this basis. Under this hypothesis (and a non-degeneracy condition that we do not discuss here, see [35]), the large time limit of the density matrix in Eq. (1) is given by the famous collapse-absorbing formula

$$\lim_{t \rightarrow \infty} \rho_t^\gamma = |e_i\rangle \langle e_i| \text{ with probability } \langle e_i, \rho_0^\gamma e_i \rangle. \quad (5)$$

This corresponds to the Born rule for measurement outcomes under projective measurements of any of the N_k at the initial time. Related results have been observed experimentally [25–27] and are proven theoretically in [31–35].

However, there are many ways to break the QND hypothesis, and we discuss three different ones:

1. *Collapse-Unitary* setup: We may allow that the Hamiltonian H is not diagonal in the pointer basis $\{|e_i\rangle\}_{i=1,\dots,d}$ related to the measurement operators $\{N_k\}_{k=1,\dots,p}$. It results then in a competition between collapse in the pointer basis and a unitary evolution (non-collapsing) generated by H .
2. *Collapse-Thermal* setup: We may take into account the thermal interactions with the external world, i.e. $L^{th} \neq 0$. Then it results in a competition between collapse Eq. (5) in the pointer basis, and, thermalisation towards a Gibbs state.
3. *Collapse-Measurement* setup: We may allow that one of the measurement operator, say N_p , is not diagonal in the pointer basis $\{|e_i\rangle\}_{i=1,\dots,d}$ related to $\{H, \{N_k\}_{k \neq p}\}$. It results then in a competition between collapse Eq. (5) in the pointer basis of $\{H, \{N_k\}_{k \neq p}\}$ and collapse in the pointer basis related to N_p , if N_p is diagonalisable. If N_p is not diagonalisable, there is competition between collapse in the pointer basis related to $\{H, \{N_k\}_{k \neq p}\}$ and the uncollapse dynamics generated by the measurement operator N_p .

In all these three setups, the large time collapse Eq. (5) is then a priori broken.

B. Strong collapse Zeno limit in a non-QND setup: Quantum jump phenomenon versus Spikes phenomenon

In this work, instead of the large time limit we consider the large γ strong collapse limit, also called the quasi-Zeno limit. For non-QND quantum trajectories, Eq. (1) leads to a richer phenomenology:

- * *Quantum jumps*: The expected quantum jumps definitively arise between the pointer basis. More

formally, the density matrix will converge to a pure jump Markov process

$$\lim_{\gamma \rightarrow \infty} \rho_t^\gamma = |X_t\rangle\langle X_t|, \quad (6)$$

where $X_t \in \{|e_i\rangle\}_{i=1,\dots,d}$ is a pure jump Markov process with explicit computable rates [39–41]. In some cases they can vanish. For example, the transition rate between pointer states decrease as $\frac{1}{|\gamma|}$ for large γ in the Collapse-Unitary setup, for a fixed H (this is reminiscent of the Zeno effect).

* *Quantum Spikes*: One finds that sharp scale-invariant fluctuations invariably decorate the jump process (see Figs. 1c, 2c and 3c below), in the limit where the measurement rate is very large. We call *quantum spikes* these seemingly instantaneous excursions. These spikes become infinitely thin when $\gamma \rightarrow \infty$, i.e. take a time $\frac{1}{|\gamma|}$ while their heights remain of order 1 in the limit. As discussed above, such spikes have been observed and explained for the case with Gaussian noise [48, 51, 52]. These articles explain the spiking phenomena as the fact that the convergence in Eq. (6) is weak. Exporting these methods in the present context seems to be a difficult task since the authors there are using tools specific to Brownian motion.

III. PRECISE SETUP: SME OF QUBIT FOR NON-DEMOLITION “RESET” CONTINUOUS MEASUREMENT OF $|-\rangle\langle-|$

We consider a qubit system with basis $\{|+\rangle, |-\rangle\}$, where continuous collapse measurement competes with a thermal, an other measurement or a unitary dynamics.

Precisely, we consider the collapse measurement of a rank one diagonal (see QND hypothesis) operator

$$N_1 = \begin{pmatrix} 0 & 0 \\ 0 & 1 \end{pmatrix} = |-\rangle\langle-|. \quad (7)$$

The jumps in the SME Eq. (1) due to the term $M_{N_1}[\rho_t^\gamma] \mathcal{N}_t^{1,\gamma}$ are, thanks to Eq. (4), given by

$$\rho \rightarrow \rho + M_{N_1}[\rho] = \frac{N_1 \rho N_1^\dagger}{\text{Tr}(N_1 \rho N_1^\dagger)} = |-\rangle\langle-|, \quad (8)$$

i.e. the result after the jump is always the same matrix, irrespective of the state just before the jump: this is a resetting dynamics [56–59]. In fact, the crucial property to get resetting dynamics is not the precise form of N_1 but the fact that the matrix N_1 is of rank one (“sharp measurement”). Since we are considering a qubit, note also that the only other rank one diagonal measurement operator satisfying QND hypothesis is

$$\begin{pmatrix} 1 & 0 \\ 0 & 0 \end{pmatrix} = |+\rangle\langle+|, \quad (9)$$

which gives exactly the same theory by the exchange $|+\rangle \rightarrow |-\rangle$. Hence our focus will be on N_1 . Note that in Section VI, we will discuss an extension to general diagonal N_1 .

By parameterising the density matrix as usual as

$$\rho_t^\gamma = \begin{pmatrix} q_t^\gamma & \bar{p}_t^\gamma \\ p_t^\gamma & 1 - q_t^\gamma \end{pmatrix}, \quad (10)$$

with $(q_t^\gamma, p_t^\gamma) \in \mathbb{R} \times \mathbb{C}$, we get explicitly in Appendix A the analytical form of the N_1 -measurement part (in the SME Eq. (1)) for general diagonal N_1 . For the particular case Eq. (7), it takes the form of a three-dimensional process:

$$\begin{cases} \dot{q}_t^\gamma = -q_t^\gamma \left(\mathcal{N}_t^{1,\gamma} - \gamma_1 \eta_1 (1 - q_t^\gamma) \right), \\ \dot{p}_t^\gamma = -\frac{\gamma_1}{2} p_t^\gamma - p_t^\gamma \left(\mathcal{N}_t^{1,\gamma} - \gamma_1 \eta_1 (1 - q_t^\gamma) \right) \end{cases}, \quad (11)$$

with

$$\mathbb{E} \left(d\mathcal{N}_t^{1,\gamma} | q_t^\gamma \right) = \gamma_1 \eta_1 (1 - q_t^\gamma) dt, \quad d\mathcal{N}_t^{1,\gamma} d\mathcal{N}_t^{1,\gamma} = d\mathcal{N}_t^{1,\gamma}.$$

Note that the resetting Eq. (8) corresponds in the coordinates Eq. (10) to the resetting to $(q = 0, p = 0)$. Moreover the equations in Eq. (11) show that the population q_t^γ is a martingale collapsing to $\{0, 1\}$ [31–35, 71]. Moreover, in average, p_t^γ shrinks trivially to zero at large time, or for strong measurement $\gamma_1 \rightarrow \infty$ (decoherence). We will study analytically three specific cases where we add either a unitary drive or a thermal bath or a non-commuting measurement.

A. Collapse-Unitary setup: Measurement of Rabi qubit coherent oscillations

We choose here no extra measurement apart from N_1 , and

$$L^{th} = 0, \quad H = k_{\gamma_1} \sigma_x = k_{\gamma_1} \begin{pmatrix} 0 & 1 \\ 1 & 0 \end{pmatrix}. \quad (12)$$

This Rabi Hamiltonian H and the measurement operator N_1 given in Eq. (7) do not commute and then, they are not diagonalisable in a common orthonormal basis. Moreover, the ad-hoc dependency in γ_1 of the Rabi frequency k_{γ_1} (which is, in general, proportional to the magnetic field) will stay unfixed for the moment, and will be discussed below in relation to the quantum Zeno effect. The Hamiltonian contribution is given by

$$-i[H, \rho_t^\gamma] = -ik_{\gamma_1} \begin{pmatrix} p_t^\gamma - \bar{p}_t^\gamma & 1 - 2q_t^\gamma \\ 2q_t^\gamma - 1 & \bar{p}_t^\gamma - p_t^\gamma \end{pmatrix}, \quad (13)$$

and the SME Eq. (1) takes then the form of a 3-dimensional piecewise deterministic Markov process

$$\begin{cases} \dot{q}_t^\gamma = -ik_{\gamma_1} (p_t^\gamma - \bar{p}_t^\gamma) - q_t^\gamma \left(\mathcal{N}_t^{1,\gamma} - \gamma_1 \eta_1 (1 - q_t^\gamma) \right) \\ \dot{p}_t^\gamma = -ik_{\gamma_1} (2q_t^\gamma - 1) - \frac{\gamma_1}{2} p_t^\gamma - p_t^\gamma \left(\mathcal{N}_t^{1,\gamma} - \gamma_1 \eta_1 (1 - q_t^\gamma) \right) \end{cases} \quad (14)$$

with

$$\mathbb{E} \left(d\mathcal{N}_t^{1,\gamma} | q_t^\gamma \right) = \gamma_1 \eta_1 (1 - q_t^\gamma) dt, \quad d\mathcal{N}_t^{1,\gamma} d\mathcal{N}_t^{1,\gamma} = d\mathcal{N}_t^{1,\gamma}.$$

Note that contrary to the Collapse-Thermal setup and the Collapse-Collapse setup, discussed in the following two sections, the real population q_t^γ is not autonomous: it depends of the complex coherence p_t^γ . Finally, when the rate of measurement vanishes (i.e. $\gamma_1 = 0$), this is the usual equation for Rabi Oscillation [72, 73]: precession of a spin one-half in an external magnetic field.

Parametrise now the density matrix in Bloch coordinates:

$$\rho_t^\gamma = \frac{1}{2} \begin{pmatrix} 1 + r_t^\gamma (\cos \theta_t^\gamma) & r_t^\gamma (\sin \theta_t^\gamma) \exp(-i\varphi_t^\gamma) \\ r_t^\gamma (\sin \theta_t^\gamma) \exp(i\varphi_t^\gamma) & 1 - r_t^\gamma (\cos \theta_t^\gamma) \end{pmatrix}, \quad (15)$$

with [74]

$$0 \leq r_t^\gamma \leq 1, \quad \theta_t^\gamma \in]-\pi, \pi], \quad \varphi_t^\gamma \in [0, \pi]. \quad (16)$$

We show in Appendix C, Eq. (C1), that in the totally efficient case $\eta_1 = 1$, Bloch sphere of pure states $r_t^\gamma = 1$ is stable under the evolution Eq. (14). We will now restrict our study to this totally efficient case and consider only pure state dynamics. We show then in Appendix C that the equation Eq. (14) takes then the form of the 2-dimensional piecewise deterministic Markov process Eq. (C3) for $(\theta_t^\gamma, \varphi_t^\gamma)$:

$$\begin{cases} \dot{\theta}_t^\gamma = (-2k_{\gamma_1} \sin(\varphi_t^\gamma) - \frac{\gamma_1}{2} \sin(\theta_t^\gamma)) + (\pi - \theta_t^\gamma) \dot{\mathcal{N}}_t^{1,\gamma}, \\ \dot{\varphi}_t^\gamma = -2k_{\gamma_1} \frac{\cos(\theta_t^\gamma)}{\sin(\theta_t^\gamma)} \cos(\varphi_t^\gamma) \end{cases} \quad (17)$$

with

$$\mathbb{E} \left(d\tilde{\mathcal{N}}_t^{1,\gamma} | \theta_t^\gamma \right) = \gamma_1 \left(\sin \frac{\theta_t^\gamma}{2} \right)^2 dt, \quad d\tilde{\mathcal{N}}_t^{1,\gamma} d\tilde{\mathcal{N}}_t^{1,\gamma} = d\tilde{\mathcal{N}}_t^{1,\gamma}.$$

Note that the Poisson noise part effect is a resetting [56–59] in the south pole of the Bloch ball $\theta = \pi$ (see Eq. (8)).

It is clear from the second equation of Eq. (17) that the plane $\varphi_t = \frac{\pi}{2}$ is stable, and then by restricting the dynamics to this plan, we see that θ_t^γ is the 1-dimensional piecewise deterministic Markov process given by

$$\dot{\theta}_t^\gamma = \left(-2k_{\gamma_1} - \frac{\gamma_1}{2} \sin(\theta_t^\gamma) \right) + (\pi - \theta_t^\gamma) \dot{\mathcal{N}}_t^{1,\gamma}. \quad (18)$$

This equation was first studied in [75] and later in [76] and will be the starting point of our analytical study in the Collapse-Unitary setup, see Section V A. Again, when $\gamma_1 = 0$, this is the usual equation for Rabi oscillations [72, 73], i.e. $\theta_t^0 = -2k_0 t$, which implies for the density matrix Eq. (15)

$$\rho_t^0 = \frac{1}{2} \begin{pmatrix} 1 + \cos(-2k_0 t) & i \sin(2k_0 t) \\ -i \sin(2k_0 t) & 1 - \cos(-2k_0 t) \end{pmatrix}. \quad (19)$$

Note finally that [75, 76] contains a different derivation of Eq. (18), by starting for a model of indirect measurement [22, 24] with 2-dimensional probes.

In Fig. 1 we show plots of the trajectory of the process for different values of γ_1 and the choice $k_{\gamma_1} = \sqrt{\omega \gamma_1}$ (a negative sign will not change the results). This scaling with γ_1 is chosen in order to see the spikes (see Appendix D for justification).

B. Collapse-Thermal setup: Measurement of thermal fluctuations

We choose here $H = 0$, no extra measurement apart from N_1 and the thermal Lindbladian in a weak coupling form [77]:

$$\begin{aligned} L^{th}[\rho] = & M_+ \rho M_+^\dagger - \frac{1}{2} M_+^\dagger M_+ \rho - \frac{1}{2} \rho M_+^\dagger M_+ \\ & + M_- \rho M_-^\dagger - \frac{1}{2} M_-^\dagger M_- \rho - \frac{1}{2} \rho M_-^\dagger M_- , \end{aligned}$$

with

$$M_+ = \sqrt{W_{-,+}} \begin{pmatrix} 0 & 1 \\ 0 & 0 \end{pmatrix}, \quad M_- = \sqrt{W_{+,-}} \begin{pmatrix} 0 & 0 \\ 1 & 0 \end{pmatrix},$$

where $W_{-,+}, W_{+,-}$ are positive coefficients characterizing the thermal bath. We use the parameterisation given in Eq. (10). The components q_t^γ of the SME Eq. (1) evolve then autonomously as a 1-dimensional piecewise deterministic Markov process defined by

$$\begin{aligned} \dot{q}_t^\gamma = & (W_{+,-} + W_{-,+}) \left(\frac{W_{-,+}}{W_{+,-} + W_{-,+}} - q_t^\gamma \right) \\ & - q_t^\gamma \left(\dot{\mathcal{N}}_t^{1,\gamma} - \gamma_1 \eta_1 (1 - q_t^\gamma) \right), \end{aligned} \quad (20)$$

with

$$\mathbb{E} \left(d\mathcal{N}_t^{1,\gamma} | q_t^\gamma \right) = \gamma_1 \eta_1 (1 - q_t^\gamma) dt, \quad d\mathcal{N}_t^{1,\gamma} d\mathcal{N}_t^{1,\gamma} = d\mathcal{N}_t^{1,\gamma}.$$

In Fig. 2 we show plots of the trajectory of the process for different values of γ_1 .

C. Collapse-Measurement setup: Competition between two measurements

We choose here $H = L^{th} = 0$ and $p = 2$ with two non-commuting reset measurement operators: the collapse measurement operator $N_1 = |-\rangle\langle -|$, with rate γ_1 , and the damping-spontaneous emission operator N_2 defined by

$$N_2 = \begin{pmatrix} 0 & 1 \\ 0 & 0 \end{pmatrix} = |+\rangle\langle -|, \quad (21)$$

acting with rate γ_2 .

Observe that N_2 does not commute with N_1 , so QND property is broken. Note that not only is it non-diagonal in the basis $|+\rangle, |-\rangle$, the matrix N_2 is in fact not diagonal in any basis. This means that even ignoring the N_1 -measurement, the measurement of N_2 does not satisfy

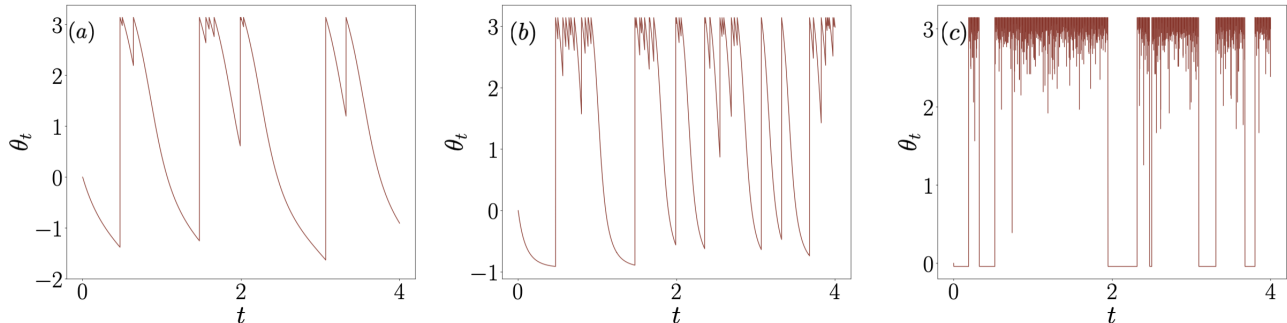


FIG. 1. Collapse-Unitary setup: Typical trajectories generated by Eq. (18) for increasing values of $\gamma_1 = 7, 25, 10000$ for (a),(b),(c) respectively, with the Rabi frequency tuned as $k_{\gamma_1} = \sqrt{\omega\gamma_1}$. In (a) we see time segments with a downward deterministic flow from π and then an upward vertical instantaneous reset to π — this constitutes a pre-spike. With increasing γ_1 , these pre-spikes either form a jump to $\theta \approx 0$ or, more often, develop into spikes. Thus we finally see in (c) a structure consisting of jumps (flows from π to $\theta \approx 0$ or instantaneous resets from $\theta \approx 0$ to π), interspersed with spikes emerging from the state $\theta = \pi$. After a jump to $\theta \approx 0$, the quantum trajectory remains here for a time $\sim 1/(4\omega)$ during which no spikes occur. In the simulations we took $\omega = 1$ and a time step $dt = 10^{-5}$ for iterating the Poisson process.

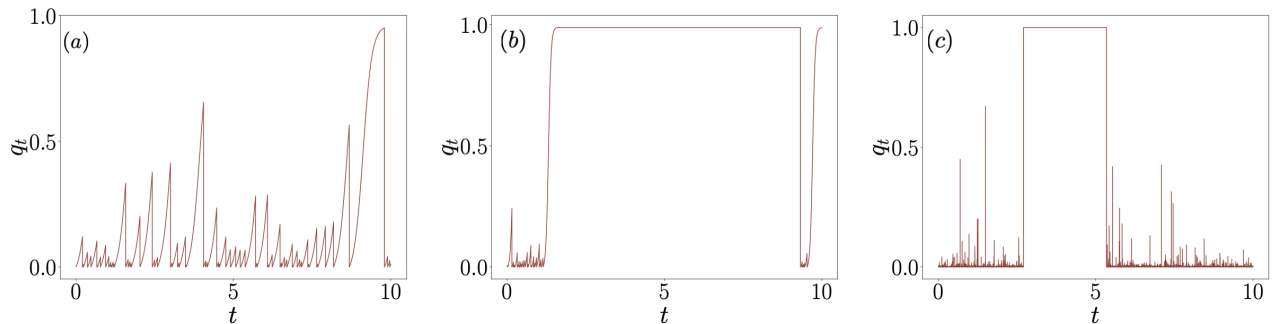


FIG. 2. Collapse-Thermal setup: Typical trajectories generated by Eq. (20) for different values of $\gamma_1 = 7, 25, 10000$ for (a),(b),(c) respectively. Here we see that in (a), the trajectory has time segments with pre-spikes which consist of an upward deterministic flow from $q = 0$, and a downward reset to the state $q = 0$. In the large γ_1 limit in (c), the pre-spikes develop into sharp spikes and we again see an effective Poisson jump process between the pointer states at $q = 0$ and $q = 1$, decorated by spikes emerging from the lower branch. The parameters here are $W_{\mp} = W_{\pm} = 0.3$, $\eta_1 = 1$, $dt = 10^{-5}$

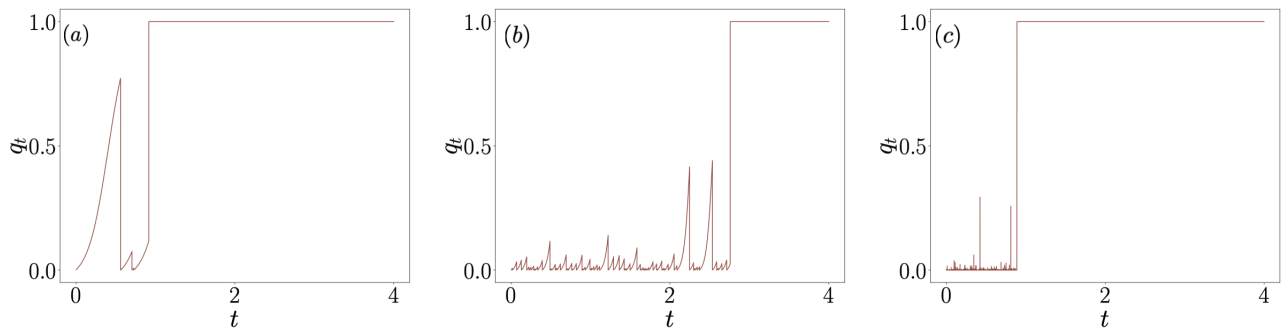


FIG. 3. Collapse-Measurement setup: Typical trajectories from Eq. (23) for increasing values of $\gamma_1 = 7, 25, 10000$ for (a),(b),(c) respectively. In this case the pre-spikes have the same form as in Fig. (2) and again we see spikes emerging in the limit of large γ_1 . However, in this case, the spikes are transient, since one has a vanishing transition rate from $q = 1$ to $q = 0$. The parameters are $\gamma_2 = 1.0$, $\eta_1 = 1.0$, $\eta_2 = 0.7$, $dt = 10^{-5}$.

the QND hypothesis and, therefore, is not by itself an a priori collapse dynamics. This is why we use the generic word ‘‘Measurement’’ in the title of this section.

Anyway, since N_2 is of rank one, the term $M_{N_2}[\rho_t^\gamma] \mathcal{N}_t^{2,\gamma}$ is a resetting dynamics to $|+\rangle\langle+|$. This is because

$$\rho \rightarrow \rho + M_{N_2}[\rho] = \frac{N_2 \rho N_2^\dagger}{\text{Tr}(N_2 \rho N_2^\dagger)} = |+\rangle\langle+|. \quad (22)$$

Hence we have here a competition between a resetting dynamics to $|-\rangle\langle-|$ induced by N_1 and a resetting dynamics to $|+\rangle\langle+|$ induced by N_2 . Note that in Section VI, we will discuss extension to more general choice of operator N_2 .

As before we use the parameterisation given in Eq. (10). The SME Eq. (1) becomes then autonomous for the diagonal (see Eq. (11) and Appendix B)

$$\begin{aligned} \dot{q}_t^\gamma &= -q_t^\gamma \left(\dot{\mathcal{N}}_t^{1,\gamma} - \gamma_1 \eta_1 (1 - q_t^\gamma) \right) \\ &+ \gamma_2 (1 - q_t^\gamma) + (1 - q_t^\gamma) \left(\dot{\mathcal{N}}_t^{2,\gamma} - \gamma_2 \eta_2 (1 - q_t^\gamma) \right), \end{aligned} \quad (23)$$

with

$$\begin{aligned} \mathbb{E} \left(d\mathcal{N}_t^{k,\gamma} | q_t^\gamma \right) &= \gamma_k \eta_k (1 - q_t^\gamma) dt, \\ d\mathcal{N}_t^{k,\gamma} d\mathcal{N}_t^{\ell,\gamma} &= \delta_{k\ell} d\mathcal{N}_t^{k,\gamma}. \end{aligned}$$

In Fig. 3, we show plots of the trajectory of the Collapse-Measurement setup for different values of γ_1 .

IV. SUMMARY OF MAIN RESULTS IN THE PRECISE SETUP

From numerical simulations (see Figs. 1, 2 and 3), we observe that, in the large γ limit, a typical trajectory is composed of two parts.

The first part is given by a pure jump Markov process with state space [78] $\{0, \pi\}$ (in the Collapse-Unitary setup) or $\{0, 1\}$ (in the Collapse-Thermal and Collapse-Measurement setups), corresponding to quantum jumps.

The second part is a decoration of this trajectory by a large number of one-sided vertical lines connecting π in the Collapse-Unitary setup (resp. 0 in the Collapse-Thermal and Collapse-Measurement setups) to random values in $(0, \pi)$ (resp. $(0, 1)$ in the Collapse-Thermal and Collapse-Measurement setups) at random times. These vertical lines correspond in fact to the deterministic trajectories (we call them pre-spikes) during successive clicks in the strong measurement limit. Our main goal now is to describe the statistics of the clicks in the strong measurement regime. Since the spikes originate only on the part of the quantum jump trajectory equal to π for the Collapse-Unitary case and 0 for the other two cases, we will focus on respectively these precise initial conditions.

As seen in Figs. 1, 2,3, for any finite γ , the pre-spikes have a specific structure consisting of a deterministic flow and a sudden reset to a particular state. In the special limit $\gamma \rightarrow \infty$, the pre-spikes become infinitely thin and occur with an infinite density (in time), and have a distribution of heights. Hence, we have a clear picture of how spikes emerge from pre-spikes. To characterize the statistic of spikes precisely, we define a spike to be localized at time t , if its tip ends at a spatial point x . We then ask for the number of spikes observed in a two-dimensional space-time box of width $(0, t)$ in time and (a, b) in space.

The probability of observing n pre-spikes, conditioned on no jumps (i.e. no pre-spikes whose tips extend to the opposite end, see Fig. 4) occurring during this time window, will be denoted by $P_c(n : t, a, b)$. To be more precise, as explained above, we focus only on initial conditions for which we can observe pre-spikes before a quantum jump, i.e. π in the Collapse-Unitary setup and 0 in the other cases. Hence, we describe the non-trivial spike statistics only during the (random) period of time in which the investigated process starts from a pointer state with spikes and does not jump to a new pointer state (without spikes) during this time period. By Markov property our analysis is in fact valid for any period of time where we really have spikes.

One of our main result of this paper is the proof, in the limit of large γ , of the Poisson distribution:

$$\lim_{\gamma \rightarrow \infty} P_c(n : t, a, b) = \frac{(\lambda_{[a,b]t})^n}{n!} \exp(-\lambda_{[a,b]t}) \quad (24)$$

$$\text{where } \lambda_{[a,b]} = \int_a^b dx I(x),$$

and the intensity for the three cases are respectively given by:

$$\begin{aligned} I(x) &= \frac{4\omega \sin(x/2)}{\cos^3(x/2)} && \text{Collapse - Unitary} \\ &= \frac{W_{-,+}}{x^2} && \text{Collapse - Thermal} \\ &= \frac{\gamma_2(1 - \eta_2)}{x^2} && \text{Collapse - Measurement.} \end{aligned} \quad (25)$$

Some comments are the following:

- In Figs. 5,6,7 we show a comparison of the above analytic forms of the three processes with computations of the mean and variance of the spike statistics obtained from numerical simulations. In all cases we see excellent agreement of the numerics with the analytic predictions.
- The first result, in the Collapse-Unitary setup, is proved only for the fully efficient case ($\eta_1 = 1$) while the latter two are valid for any non-vanishing efficiency ($0 < \eta_1 \leq 1$). Anyway, numerical simulation of the inefficient case ($0 < \eta_1 < 1$) in the Collapse-Unitary set-up (i.e. equation Eq. (14)) show that the spikes exist anyway in the non-autonomous q process (See Fig. 8).

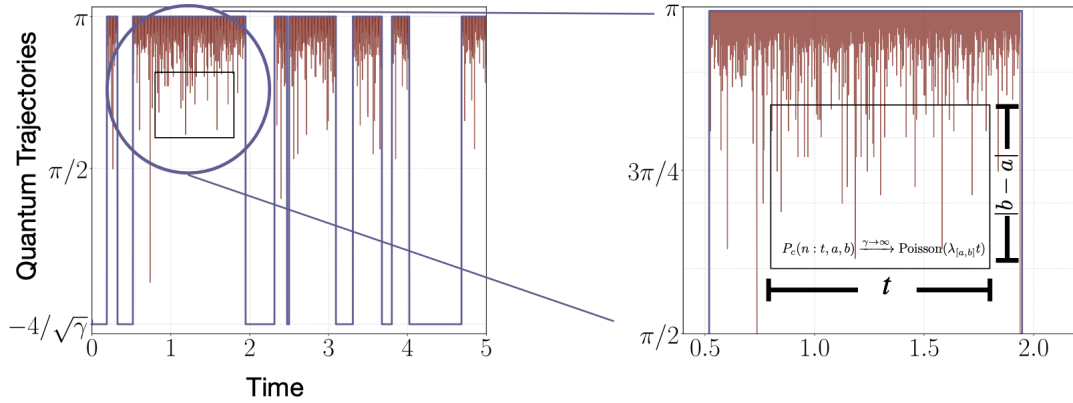


FIG. 4. Pictorial depiction of the construction of $P_c(n : t, a, b)$: the probability of observing n pre-spikes, given that there are no jumps in between. Quantum trajectories are characterized by quantum jumps (shown in violet) and are accompanied by spikes (shown in brown). The spike statistics occurring between consecutive jumps within a black box of width $|b - a|$ and length t is the focus of this article. It is anticipated that at large measurement strength, these spike statistics follows a Poisson distribution.

- By a change of variable $q = (1 + \cos x)/2$ for the first case, all three intensities acquire the same universal form. This change of variable is in fact natural since it corresponds to returning to the representation of the qubit in Eq. (10) with the inverse of the change of variable given by Eq. (15). Interestingly, the spikes statistics above are similar to the spikes statistics obtained in [48, 51, 52, 54], in the case where the noise \mathcal{N} is not Poissonian, but Gaussian.
- In the Collapse-Measurement setup, for a perfect measurement efficiency of N_2 (i.e. $\eta_2 = 1$), the spikes disappear completely, indicating a complex interplay of measurement of two non-commuting observables in non-QND measurement.
- In these three cases, the jump transition rates of the jump process can be computed explicitly. In the Collapse-Unitary setup, the jumps between the two pointer states occur with rate 4ω while in the Collapse-Thermal setup, the jumps between the states occur with rates $W_{-,+}$ and $W_{+,-}$ respectively, and in the Collapse-Measurement setup, only transitions are one-sided with rate γ_2 (parameters are specified in Sec. III).

V. MATHEMATICAL DERIVATIONS

A. Study in the Collapse-Unitary setup

To simplify notation, we denote γ_1 by γ and $\tilde{\mathcal{N}}^{1,\gamma}$ by \mathcal{N} , θ^γ by θ . We also choose $k_\gamma = \sqrt{\omega\gamma}$ in order to get quantum spikes in the large γ limit (see Appendix D for justification). The dynamics is then specified by the

following stochastic evolution equation (see Eq. (18)):

$$d\theta_t = \Omega(\theta_t) dt + (\pi - \theta_t) d\mathcal{N}_t, \quad (26)$$

where the drift term $\Omega := \Omega^\gamma$ and the Poissonian noise \mathcal{N}^γ satisfy:

$$\Omega(\theta) = -2\sqrt{\omega\gamma} \left[1 + \sqrt{\frac{\gamma}{16\omega}} \sin \theta \right], \quad (27)$$

$$\mathbb{E}[d\mathcal{N}_t|\theta_t] = \alpha(\theta_t) dt := \gamma \sin^2 \frac{\theta_t}{2} dt. \quad (28)$$

Hence the dynamics evolves deterministically in $(\theta^* = -\sin^{-1}(4\sqrt{\omega/\gamma}), \pi)$ but at some random times prescribed by \mathcal{N} , the angle is resetting to the value π , i.e., a "click" occurs. Rarely, during the deterministic evolution, no resetting occurs and the trajectory is able to reach θ^* and is stuck around θ^* for a random time until a new resetting to π occurs. In the large γ limit, as $\theta^* \rightarrow 0$, we say then that we have a jump from π to 0 and afterwards a jump (instantaneous) from 0 to π .

With the notations of [76], the situation considered here corresponds then to the special case $\gamma_0 = \sqrt{\omega\gamma}$, or equivalently $\lambda = \gamma/(4\gamma_0) = \sqrt{\frac{\gamma}{16\omega}}$. We recall that we are interested in the strong measurement regime $\gamma \rightarrow \infty$, not investigated in [76]. Hence, the angle $\hat{\theta}_t$, evolving according to the deterministic equation

$$d\hat{\theta}_t = \Omega(\hat{\theta}_t) dt, \quad (29)$$

is confined to the range $(-\sin^{-1}(1/\lambda), \pi) \approx (-4\sqrt{\omega/\gamma}, \pi)$, the last approximation being valid since γ is large. In particular, for $t \geq 0$, we have the exact solution [79]:

$$\tan\left(\frac{\hat{\theta}_t(0|\pi)}{2}\right) = -\frac{\sinh(\beta\sqrt{\omega\gamma} t - \phi)}{\sinh(\beta\sqrt{\omega\gamma} t)}, \quad (30)$$

where

$$\beta = \sqrt{\frac{\gamma}{16\omega} - 1} = \sinh(\phi). \quad (31)$$

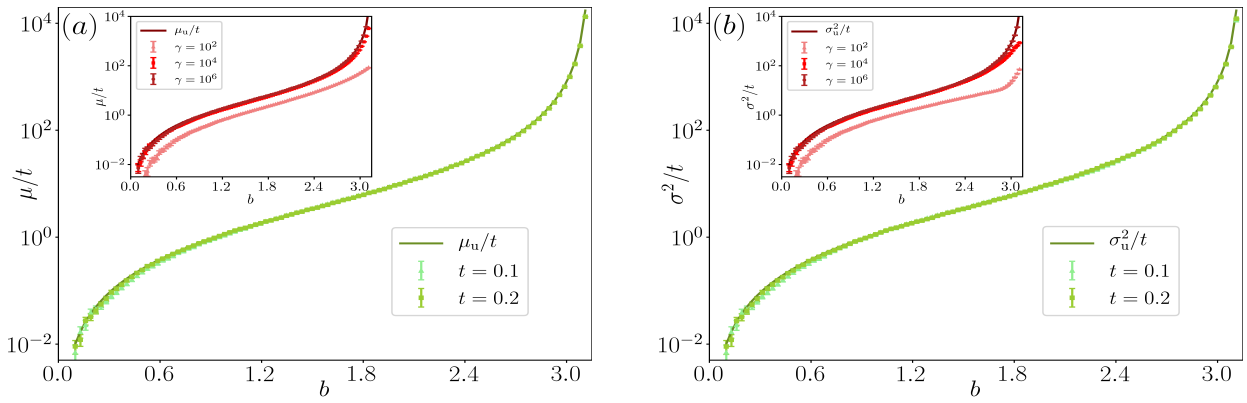


FIG. 5. Collapse-Unitary case: (a) Mean (b) Variance of the distribution (conditioned on no-jumps) of the number of spikes (from $\theta_t = \pi$) per unit time in a space-time box $(0, b) \times (0, t)$ plotted against the box edge b for $\gamma = 10^6$. The data-points were obtained for $\omega = 1$ by averaging over 10^4 realizations. μ_u and σ_u^2 are the mean and variance, respectively, of the theoretically-predicted Poisson process in Eq. (24). The data in the insets, plotted for a fixed time $t = 0.1$, converge to μ_u/t and σ_u^2/t at large γ .

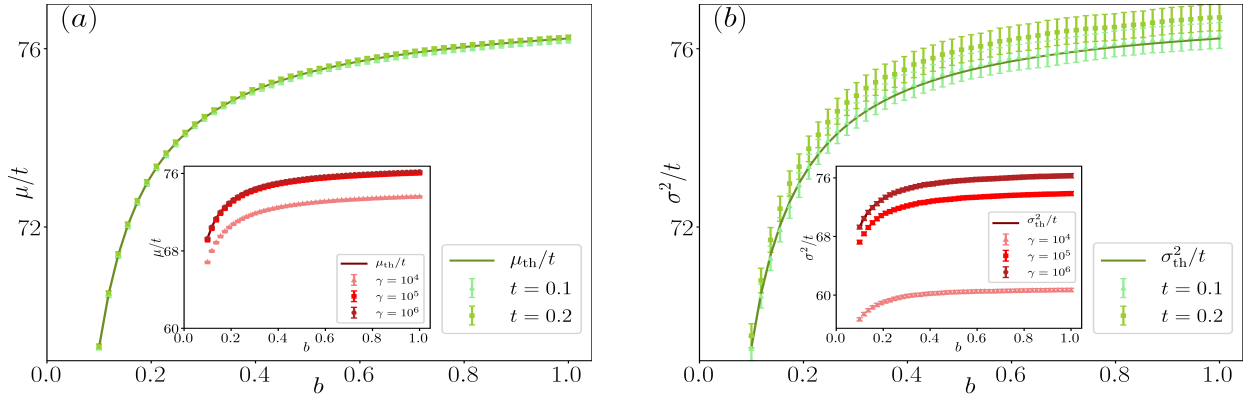


FIG. 6. Collapse-Thermal case: (a) Mean (b) Variance of the distribution (conditioned on no-jumps) of the number of spikes (from $q_t = 0$) per unit time in a space-time box $(0.01, b) \times (0, t)$ plotted against the box edge b for $\gamma = 10^6$. The data-points were obtained for the parameters $W_{-,+} = 0.77$, $W_{+,-} = 0.23$ by averaging over 10^5 realizations. μ_{th} and σ_{th}^2 are the mean and variance, respectively, of the theoretically-predicted Poisson process in Eq. (24). The data in the insets, plotted for a fixed time $t = 0.1$, converge to μ_{th}/t and σ_{th}^2/t at large γ .

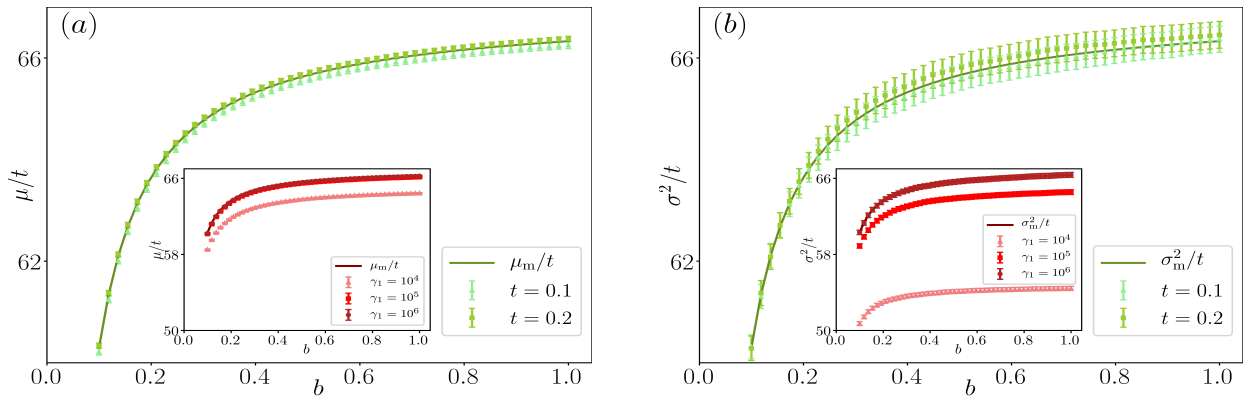


FIG. 7. Collapse-Measurement case: (a) Mean (b) Variance of the distribution (conditioned on no-jumps) of the number of spikes (from $q_t = 0$) per unit time in a space-time box $(0.01, b) \times (0, t)$ plotted against the box edge b for $\gamma_1 = 10^6$. The data-points were obtained for the parameters $\gamma_2 = 1$ and $\eta_1 = \eta_2 = 0.33$ by averaging over 10^5 realizations. μ_m and σ_m^2 are the mean and variance, respectively, of the theoretically-predicted Poisson process in Eq. (24). The data in the insets, plotted for a fixed time $t = 0.1$, converge to μ_m/t and σ_m^2/t at large γ_1 .

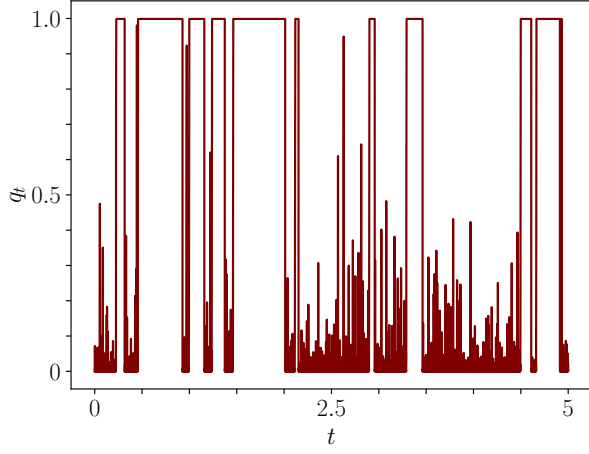


FIG. 8. Typical trajectories for Collapse-Unitary setup for inefficient measurements, for the parameters $\eta_1 = 0.33$, $\gamma = 10^4$ and $\omega = 1$. Similar to the Collapse-Thermal and Collapse-Measurement cases, the jumps between $q_t = 0$ and $q_t = 1$ are interspersed with spikes from $q_t = 0$ in the strong measurement limit.

Let τ be the time taken by a deterministic trajectory $\hat{\theta}$ to evolve from $\hat{\theta}_0 = \pi$ to $\hat{\theta}_\tau = 0$. From Eq. (30), we note $\tau = \phi/(\beta\sqrt{\omega\gamma})$. For $\gamma \gg 1$, $\tau \approx 2 \log \gamma/\gamma$. If $c \in (0, \pi)$, let us also denote the time for the deterministic dynamics to reach c when starting from π by τ_c . A straightforward inversion of Eq. 30 yields

$$\tau_c = \frac{1}{2\beta\sqrt{\omega\gamma}} \log \left[1 + \frac{2\beta}{\tan(c/2) + e^{-\phi}} \right]. \quad (32)$$

Consider the probability, $p_0^t(t_1, t_2, \dots, t_n | \theta_0)$, given that at initial time the state is θ_0 , to see a sequence of n clicks occurring exactly at times $t_1 < t_2 < \dots < t_n$ in the time interval $(0, t)$ and that no jump occurs during the time interval $(0, t)$ (no-jump condition), meaning $\tau \geq t_j - t_{j-1}$ for any $j \leq n$. Given the clicks, the quantum trajectory becomes deterministic and say is given by $\{\theta_0, \theta_{t_1}, \pi, \theta_{t_2}, \pi, \dots, \theta_{t_n}, \pi, \theta_t\}$. The evolution from $\theta_0 \rightarrow \theta_{t_1}$, $\pi \rightarrow \theta_{t_i}$ (for $i = 2, \dots, n$) and $\pi \rightarrow \theta_t$ are given by the deterministic flow in Eq. (29).

Let us define $\mu(\Delta t | \theta_i)$ as the probability to not have a click during the time interval Δt for the initial condition $\theta = \theta_i$. This is given by

$$\mu(\Delta t | \theta_i) = e^{-\int_0^{\Delta t} ds \alpha(\hat{\theta}_s(0 | \theta_i))} = \frac{\Omega(\theta_i)}{\Omega(\hat{\theta}_{\Delta t}(0 | \theta_i))} e^{-\frac{\gamma \Delta t}{2}}. \quad (33)$$

Then we have:

$$\begin{aligned} & p_0^t(t_1, t_2, \dots, t_n | \hat{\theta}_0) \\ &= \mu(t_1 | \theta_0) \alpha(\hat{\theta}_{t_1}) \prod_{i=2}^n [\mu(t_i - t_{i-1} | \pi) \alpha(\hat{\theta}_{t_i - t_{i-1}}(0 | \pi))] \\ & \times \mu(t - t_n | \pi). \end{aligned} \quad (34)$$

Using the explicit solution in Eq. (30) and after some algebra we get:

$$\begin{aligned} \mu(t | \pi) \alpha(\hat{\theta}_t(0 | \pi)) &= \frac{\gamma \sinh^2(\beta\sqrt{\omega\gamma}t - \phi)}{\beta^2}, \\ \mu(t | \pi) &= \frac{\sinh^2(\beta\sqrt{\omega\gamma}t) + \sinh^2(\beta\sqrt{\omega\gamma}t - \phi)}{\beta^2}. \end{aligned} \quad (35)$$

The joint probability $P_j(n : t, a, b)$ to observe exactly n pre-spikes in the time interval $[0, t]$ and in the space interval $[a, b]$ (where $0 < a < b < \pi$), starting from π , and such that no jumps occur in the time interval $[0, t]$, is given by

$$\begin{aligned} & P_j(n : t, a, b) \\ &= \sum_{m=0}^{\infty} \frac{(n+m)!}{n!m!} \prod_{i=1}^{n+m} \int_0^{t_{i+1}} dt_i p_0^t(t_1, t_2, \dots, t_{n+m} | \pi) \\ & \times \prod_{j=1}^m [\Theta(\tau_b - (t_j - t_{j-1})) + \Theta((t_j - t_{j-1}) - \tau_a)] \\ & \times \prod_{j=1}^n \Theta((t_j - t_{j-1}) - \tau_b) \Theta(\tau_a - (t_j - t_{j-1})) \\ & \times \prod_{j=1}^{n+m} \Theta(\tau - (t_j - t_{j-1})) \Theta(\tau - (t - t_{n+m})), \end{aligned} \quad (36)$$

where we have defined $t_{n+m+1} = t$ and Θ is the Heaviside function. Taking time-Laplace transform $\hat{P}_j(n : \sigma, a, b) = \int_0^\infty dt e^{-\sigma t} P_j(n : t, a, b)$ gives

$$\hat{P}_j(n : \sigma, a, b) = \sum_{m=0}^{\infty} \frac{(n+m)!}{n!m!} C^m(\sigma) D^n(\sigma) E(\sigma), \quad (37)$$

where

$$\begin{aligned} C(\sigma) &= \int_0^\infty dt \mu(t | \pi) \alpha(\hat{\theta}_t(0 | \pi)) [\Theta(\tau_b - t) + \Theta(t - \tau_a)] \\ & \times \Theta(\tau - t) e^{-\sigma t}, \\ D(\sigma) &= \int_0^\infty dt \mu(t | \pi) \alpha(\hat{\theta}_t(0 | \pi)) \Theta(\tau_a - t) \Theta(t - \tau_b) e^{-\sigma t}, \\ E(\sigma) &= \int_0^\infty dt \mu(t | \pi) \Theta(\tau - t) e^{-\sigma t}. \end{aligned} \quad (38)$$

Performing the summation, we get

$$\hat{P}_j(n : \sigma, a, b) = \frac{D^n(\sigma) E(\sigma)}{[1 - C(\sigma)]^{1+n}}. \quad (39)$$

Writing the generating function ($0 \leq s \leq 1$)

$$Z(s : \sigma, a, b) = \sum_{n=0}^{\infty} s^n \hat{P}_j(n : \sigma, a, b), \quad (40)$$

we find the exact formula

$$Z(s : \sigma, a, b) = \frac{E(\sigma)}{1 - C(\sigma) - sD(\sigma)}. \quad (41)$$

Thanks to the explicit expressions Eq. (35), the functions $C(\sigma)$, $D(\sigma)$ and $E(\sigma)$ can be computed explicitly and their asymptotic behaviour for large γ can be obtained (See Appendix E for details). It follows that for any $s \in [0, 1]$ fixed we have in the large γ limit that

$$Z(s : \sigma, a, b) \approx \frac{1}{\sigma + 4\omega + 4\omega(1-s)[\tan^2(b/2) - \tan^2(a/2)]}. \quad (42)$$

The probability $S(t)$ of no jump occurring from π to 0 in the time interval $(0, t)$ is obtained by taking $s = 1$ in the generating function in Eq. (42), which yields $S(t) = e^{-4\omega t}$. Since $1 - S(t)$ is the cumulative distribution function of the distribution of time of first passage from π to 0, this implies that the first time to reach 0 is exponentially distributed with a mean equal to $1/(4\omega)$. The probability $P_c(n : t, a, b)$ to observe exactly n pre-spikes in the time interval $[0, t] \times [a, b]$, given that no jump occurs in the time interval $[0, t]$, can be obtained by

$$P_c(n : t, a, b) = \frac{P_j(n : t, a, b)}{S(t)},$$

which is given by the Poisson distribution in the large γ limit (as announced in Eq. (24)),

$$\frac{(\lambda_{[a,b]}t)^n e^{-\lambda_{[a,b]}t}}{n!}, \quad \text{where } \lambda_{[a,b]} = \int_a^b dx \frac{4\omega \sin(x/2)}{\cos^3(x/2)}. \quad (43)$$

Moreover, by using Eq. (33) and (30) we have that the probability to have no resetting to π by starting from 0 in a time interval of length Δt is given by

$$\mu(\Delta t|0) = \frac{-2\sqrt{\omega\gamma}e^{-\frac{\gamma\Delta t}{2}}}{\Omega\left(-2\tan^{-1}\left(\frac{\sinh(\beta\sqrt{\omega\gamma}\Delta t)}{\sinh(\beta\sqrt{\omega\gamma}\Delta t + \phi)}\right)\right)}. \quad (44)$$

By performing the expansion in γ we get that

$$\mu(\Delta t|0) \approx \exp(-4\omega\Delta t), \quad (45)$$

so that the time to be resetting to π when starting from 0 is also exponentially distributed with mean $1/(4\omega)$.

B. Study in the Collapse-Thermal setup

To simplify notation, we denote γ_1 by γ and $\mathcal{N}^{1,\gamma}$ by \mathcal{N} , q_t^γ by q_t . Eq. (20) can then be rewritten as

$$dq_t = \Omega(q_t)dt - q_t d\mathcal{N}_t, \quad (46)$$

where the quadratic drift term Ω and the rate function α of \mathcal{N}_t are given by:

$$\begin{aligned} \Omega(q) &= W_{-,+} - q(W_{+,-} + W_{-,+} - \gamma\eta) - \gamma\eta q^2, \\ \mathbb{E}[d\mathcal{N}_t|q_t] &= \alpha(q_t)dt = \gamma\eta(1 - q_t)dt. \end{aligned} \quad (47)$$

The roots of $\Omega(q)$ are the fixed points of the no-click deterministic dynamics, given by

$$q_{\pm} = \frac{\gamma\eta - W_{+,-} - W_{-,+} \pm \sqrt{(W_{+,-} + W_{-,+} - \gamma\eta)^2 + 4W_{-,+}\gamma\eta}}{2\gamma\eta},$$

which are always real and distinct. Note that $q_- < 0 < q_+$, provided all the parameters are not identically zero. For an initial condition $q_0 < q_+$, the stochastic dynamics is confined to $[0, q_+)$ for $\gamma \gg 1$.

The solution of the deterministic equation $d\hat{q}_t = \Omega(\hat{q}_t)dt$ starting from q_0 is given by

$$\hat{q}_t(q_0) = \frac{q_+(q_0 - q_-) + q_-(q_+ - q_0)e^{-\gamma\eta(q_+ - q_-)t}}{(q_0 - q_-) + (q_+ - q_0)e^{-\gamma\eta(q_+ - q_-)t}}. \quad (48)$$

For $c \in [0, 1]$, let τ_c be the time taken to evolve from $q_0 = 0$ to $q = c$. A straightforward inversion of Eq. (48) shows that

$$\tau_c = \frac{1}{\gamma\eta(q_+ - q_-)} \log \left| \frac{(c - q_-)q_+}{q_-(q_+ - c)} \right|, \quad (49)$$

and let τ be the time taken by a deterministic trajectory to evolve from $q = 0$ to $q = 1$. For $\gamma \gg 1$,

$$\tau \sim \frac{1}{\gamma\eta} \log \frac{\gamma^2 \eta^2}{W_{+,-}W_{-,+}}.$$

Similar to the Collapse-Unitary case, we explicitly obtain the functions

$$\begin{aligned} \mu(t|q_0) &= e^{-\int_0^t ds \alpha[\hat{q}_s(q_0)]} \\ &= \frac{(q_0 - q_-)e^{-\gamma\eta(1-q_+)t} + (q_+ - q_0)e^{-\gamma\eta(1-q_-)t}}{q_+ - q_-}, \\ \mu(t|q_0)\alpha[q_t(q_0)] &= \frac{\gamma\eta}{q_+ - q_-} \left[(q_0 - q_-)(1 - q_+)e^{-\gamma\eta(1-q_+)t} + \right. \\ &\quad \left. (q_+ - q_0)(1 - q_-)e^{-\gamma\eta(1-q_-)t} \right]. \end{aligned} \quad (50)$$

which we plug into the Eq. (38) to explicitly obtain the functions $C(\sigma)$, $D(\sigma)$ and $E(\sigma)$ and obtain their asymptotic behaviour for large γ (See Appendix E for details).

Consider the probability, $P_j(n : t, a, b)$, to observe exactly n pre-spikes in the time interval $[0, t]$ and in the space interval $[a, b]$ (where $0 < a < b < 1$), and that no jump occurs in the time interval $[0, t]$, starting from 0. The corresponding generating function in the Laplace domain $Z(s : \sigma, a, b)$, defined in Eq. (40), can be obtained

by plugging $C(\sigma)$, $D(\sigma)$ and $E(\sigma)$ into Eq. (41). It follows that for any $s \in [0, 1]$ fixed we have in the large γ limit that

$$\lim_{\gamma \rightarrow \infty} Z(s : \sigma, a, b) = \frac{1}{\sigma + W_{-,+} + W_{-,+}(1-s) \left(\frac{1}{a} - \frac{1}{b} \right)}. \quad (51)$$

The probability $S(t)$ of no jump occurring from 0 to 1 in the time interval $(0, t)$ is obtained by taking $s = 1$ in the generating function in Eq. (42), which yields $S(t) = e^{-W_{-,+}t}$. This implies that the first time to reach 1 starting from 0 is exponentially distributed with a mean equal to $1/W_{-,+}$. The probability $P_c(n : t, a, b)$ to observe exactly n spikes in the time interval $[0, t] \times [a, b]$, given that no jump occurs in the time interval $[0, t]$, can be obtained by

$$P_c(n : t, a, b) = \frac{P_j(n : t, a, b)}{S(t)},$$

which is given by the Poisson distribution in the large γ limit (as announced in Eq. (24)),

$$\frac{(\lambda_{[a,b]}t)^n e^{-\lambda_{[a,b]}t}}{n!}, \quad \text{where } \lambda_{[a,b]} = \int_a^b dx \frac{W_{-,+}}{x^2}. \quad (52)$$

Moreover, similar to the Collapse-Unitary setup, we have that the probability to have no resetting to 0 by starting from 1 in a time interval of length Δt is given for large γ by

$$\mu(\Delta t|1) \approx \exp(-W_{+,-}\Delta t), \quad (53)$$

so that the time to be resetting to 0 when starting from 1 is exponentially distributed with mean $1/W_{+,-}$.

C. Study in the Collapse-Measurement setup

To simplify notation, we denote \mathcal{N}^{1,γ_1} by \mathcal{N}^1 , \mathcal{N}^{2,γ_2} by \mathcal{N}^2 and q_t^γ by q_t . Eq. (23) can then be rewritten as

$$dq_t = \Omega(q_t) dt - q_t d\mathcal{N}_t^1 + (1 - q_t) d\mathcal{N}_t^2, \quad (54)$$

where the quadratic drift term $\Omega := \Omega^{\gamma_1, \gamma_2}$ and the rate functions α of \mathcal{N}_t^1 and $\tilde{\alpha}$ of \mathcal{N}_t^2 are given by:

$$\begin{aligned} \Omega(q) &= (\gamma_2 + q\gamma_1\eta_1)(1-q) - \gamma_2\eta_2(1-q)^2, \\ \mathbb{E}(d\mathcal{N}_t^1|q_t) &= \alpha(q_t) dt = \gamma_1\eta_1(1-q_t)dt, \\ \mathbb{E}(d\mathcal{N}_t^2|q_t) &= \tilde{\alpha}(q_t) dt = \gamma_2\eta_2(1-q_t)dt. \end{aligned} \quad (55)$$

The roots of $\Omega(q)$ are the fixed points of the no-click dynamics, given by

$$q_- = \frac{\gamma_2(\eta_2-1)}{\gamma_2\eta_2+\gamma_1\eta_1}, \quad q_+ = 1. \quad (56)$$

Note that $q_- < 0$ (provided N_2 is not measured with unit efficiency).

The solution of the deterministic equation $d\hat{q}_t = \Omega(\hat{q}_t)dt$, starting from q_0 at time $t = 0$, is given by

$$\hat{q}_t(q_0) = \frac{(q_0 - q_-) + q_-(1 - q_0)e^{-(\gamma_1\eta_1 + \gamma_2\eta_2)(1-q_-)t}}{(q_0 - q_-) + (1 - q_0)e^{-(\gamma_1\eta_1 + \gamma_2\eta_2)(1-q_-)t}}. \quad (57)$$

For $c \in [0, 1]$, let τ_c be the time taken to evolve from $q_0 = 0$ to $q = c$. A straightforward inversion of Eq. (57) show that

$$\tau_c = \frac{1}{(\eta_1\gamma_1 + \eta_2\gamma_2)(1-q_-)} \log \left| \frac{(c - q_-)}{q_-(1-c)} \right|. \quad (58)$$

Let τ be the time taken by a deterministic trajectory to evolve from $q = 0$ to $q = 1 - \epsilon$. For $\gamma_1 \gg 1$,

$$\tau \sim \frac{1}{\gamma_1\eta_1} \log \left| \frac{\gamma_1\eta_1}{\epsilon\gamma_2(\eta_2-1)} \right|.$$

Similar to the Collapse-Unitary and Collapse-Thermal cases, we explicitly obtain the functions

$$\begin{aligned} \mu(t|q_0) &= e^{-\int_0^t ds (\alpha[\hat{q}_s(q_0)] + \tilde{\alpha}[\hat{q}_s(q_0)])}, \\ &= \frac{(q_0 - q_-) + (1 - q_0)e^{-(\gamma_1\eta_1 + \gamma_2\eta_2)(1-q_-)t}}{1 - q_-}, \\ \mu(t|q_0)\alpha[\hat{q}_t(q_0)] &= \gamma_1\eta_1(1 - q_0)e^{-(\gamma_1\eta_1 + \gamma_2\eta_2)(1-q_-)t}, \end{aligned} \quad (59)$$

which we plug into the Eq. (38) to explicitly obtain the functions $C(\sigma)$, $D(\sigma)$ and $E(\sigma)$ and obtain their asymptotic behaviour for large γ (See Appendix E for details).

Consider the probability, $P_j(n : t, a, b)$, to observe exactly n pre-spikes in the time interval $[0, t]$ and in the space interval $[a, b]$ (where $0 < a < b < 1$), and that no jump occurs in the time interval $[0, t]$, starting from 0. The corresponding generating function in the Laplace domain $Z(s : \sigma, a, b)$, defined in Eq. (40), can be obtained by plugging $C(\sigma)$, $D(\sigma)$ and $E(\sigma)$ into Eq. (41). It follows that for any $s \in [0, 1]$ fixed we have in the large γ_1 limit (for γ_2 fixed)

$$\lim_{\gamma_1 \rightarrow \infty} Z(s : \sigma, a, b) = \frac{1}{\sigma + \gamma_2 + (1-s)\gamma_2(1-\eta_2) \left(\frac{1}{a} - \frac{1}{b} \right)}. \quad (60)$$

The probability $S(t)$ of no jump occurring from 0 to 1 in the time interval $(0, t)$ is obtained by taking $s = 1$ in the generating function in Eq. (42), which yields $S(t) = e^{-\gamma_2 t}$. This implies that the first time to reach 1 starting from 0 is exponentially distributed with a mean equal to $1/\gamma_2$ and that the statistics of the spikes given the no-jump condition is given by the Poisson distribution in the large γ_1 limit (as announced in Eq. (24)),

$$\frac{(\lambda_{[a,b]}t)^n e^{-\lambda_{[a,b]}t}}{n!}, \quad \text{where } \lambda_{[a,b]} = \int_a^b dx \frac{\gamma_2(1-\eta_2)}{x^2}. \quad (61)$$

Note that, in this setup, the probability to have resetting to 0 by starting from 1 vanishes and the flow term out of 1 also vanishes. The mean time of first passage from 0 to 1 is γ_2^{-1} and hence, spikes are typically not observed for $t \gg \gamma_2^{-1}$.

VI. GENERALIZATION: A GENERAL PERSPECTIVE ON SPIKES IN 1D PIECEWISE DETERMINISTIC MARKOV PROCESS

Our interest in spikes processes was motivated by quantum physics and its analytical description was limited by various technicalities. But we may enlarge the discussion to cover other physical situations of interest.

To this end, let us consider a piecewise 1-dimensional Markov process $(q_t^\gamma)_{t \geq 0}$ evolving according to the SDE

$$\dot{q}_t^\gamma = F(q_t^\gamma) + G(q_t^\gamma) \left(\dot{\mathcal{N}}_t^\gamma - \gamma H(q_t^\gamma) \right), \quad (62)$$

where \mathcal{N}^γ is a Poisson process satisfying

$$\mathbb{E}(d\mathcal{N}_t^\gamma | q_t^\gamma) = \gamma H(q_t^\gamma) dt, \quad d\mathcal{N}_t^\gamma d\mathcal{N}_t^\gamma = d\mathcal{N}_t^\gamma.$$

We assume that

$$G(0)H(0) = 0 = G(1)H(1), \quad F(0) \geq 0, \quad F(1) \leq 0, \quad (63)$$

so that the process q^γ takes values in $[0, 1]$. We conjecture that the graph $\{(t, q_t^\gamma) ; t \geq 0\}$ of the process q^γ converges as $\gamma \rightarrow \infty$ to the random time-space ‘‘spike’’ graph \mathbb{Q} , which can be described as follows.

Let $(\bar{q}_t)_{t \geq 0}$ be the continuous pure jump Markov process on $\{0, 1\}$ with rate $F(0)$ (resp. $F(1)$) to jump from 0 to 1 (resp. from 1 to 0). The process \bar{q} can be seen as the first rough description of q^γ for large γ , but it misses a more refined structure of the limit of q^γ .

‘‘Decorate’’ then the trajectory \bar{q} with spikes, which are vertical intervals (in space) included in $[0, 1]$, distributed as

$$\mathbb{Q}_t = \begin{cases} [0, M_t], & \bar{q}_{t-} = \bar{q}_t = 0, \\ [M_t, 1], & \bar{q}_{t-} = \bar{q}_t = 1, \\ [0, 1], & \bar{q}_{t-} \neq \bar{q}_t, \end{cases} \quad (64)$$

where, given the trajectory \bar{q} , $(t, M_t)_{t \geq 0}$ is the time-space Poisson process on $[0, \infty) \times [0, 1]$.

More precisely, the spikes from 0 to 1 have intensity $|F(0)| \mathbf{1}_{H(0) \neq 0} \frac{dt dx}{x^2} \mathbf{1}_{x \in [0, 1]}$ and the spikes from 1 to 0 have intensity $|F(1)| \mathbf{1}_{H(1) \neq 0} \frac{dt dx}{(1-x)^2} \mathbf{1}_{x \in [0, 1]}$.

More explicitly, let $P_c[n : (s, t), a, b]$ be the probability of observing n tips of pre-spikes belonging to (a, b) , conditioned on no jumps occurring during the time window (s, t) . Its large γ limit corresponds precisely to a Poisson distribution limit with parameter: $\lambda_{[a, b]}^{\bar{q}}(t-s)$,

$$\text{i.e.} \quad \lim_{\gamma \rightarrow \infty} P_c[n : (s, t), a, b] = \frac{(t-s)^n}{n!} e^{-\lambda_{[a, b]}^{\bar{q}}(t-s)}, \quad (65)$$

with the intensity parameter given by

$$\lambda_{[a, b]}^{\bar{q}} = \begin{cases} \int_a^b dx \frac{|F(0)| \mathbf{1}_{H(0) \neq 0}}{x^2} & \text{if } \bar{q} \big|_{[s, t]} = 0, \\ \int_a^b dx \frac{|F(1)| \mathbf{1}_{H(1) \neq 0}}{(1-x)^2} & \text{if } \bar{q} \big|_{[s, t]} = 1. \end{cases}$$

Observe also that in this general context (not motivated by quantum physics), to adapt the analytical proofs developed in this paper, we would need:

1. to have a resetting dynamics, i.e. $G(q) = q^* - q$, $q^* \in (0, 1)$;
2. to have a good understanding of the deterministic flow \hat{q}^γ defined by $\dot{\hat{q}}_t^\gamma = F(\hat{q}_t^\gamma) - \gamma G(\hat{q}_t^\gamma) H(\hat{q}_t^\gamma)$ for large γ .

Note that the Collapse-Unitary case considered in section IV and V A is not in the form of our general set-up Eq. (62) on $[0, 1]$. To transform Eq. (18) to an equation on the line as in Eq. (62), we need to come back to the usual coordinate q^γ in equation Eq. (14). With the notations of Section IV, the plane $\varphi_t = \frac{\pi}{2}$ is stable, and then by restricting the dynamics to this plane, we find the equation

$$\dot{q}_t^\gamma = F_\gamma(q_t^\gamma) + G(q_t^\gamma) \left(\dot{\mathcal{N}}_t^\gamma - \gamma H(q_t^\gamma) \right), \quad (66)$$

with

$$F_\gamma(q) = 2k_\gamma \sqrt{q(1-q)}, \quad G(q) = -q, \quad H(q) = \eta(1-q),$$

and \mathcal{N}^γ is a Poisson process satisfying

$$\mathbb{E}(d\mathcal{N}_t^\gamma | q_t^\gamma) = \gamma H(q_t^\gamma) dt, \quad d\mathcal{N}_t^\gamma d\mathcal{N}_t^\gamma = d\mathcal{N}_t^\gamma. \quad (67)$$

At first sight, the equation Eq. (66) is directly in the form Eq. (62) if k_γ is γ independent, but then the general previous conjecture gives that there are no jumps and no spikes because $F(0) = 0 = F(1)$ in Eq. (67) (Zeno effect). On the other hand, if $k_\gamma = \sqrt{\omega\gamma}$ as we did in section IV and V A, then $F_\gamma(q) = 2\sqrt{\gamma}\sqrt{\omega q(1-q)}$ and the factor $\sqrt{\gamma}$ breaks the validity of the conjecture.

Below we first give, in Sec. VI A some non-quantum motivated examples where we numerically verify the above conjecture. In Sec. VI B we discuss a non-trivial quantum example where we expect the conjecture to be true but our analytical approach based on resetting cannot be applied. Finally in Sec. VI C we discuss a generalization of Eq. (62) in the context of collapse-measurement set-up.

A. Example 1 with resetting: Non-Quantum SDEs

In the general Markovian 1D piecewise deterministic process given by Eq. (62), we numerically study the emergence of spikes for large γ . In the context of resetting

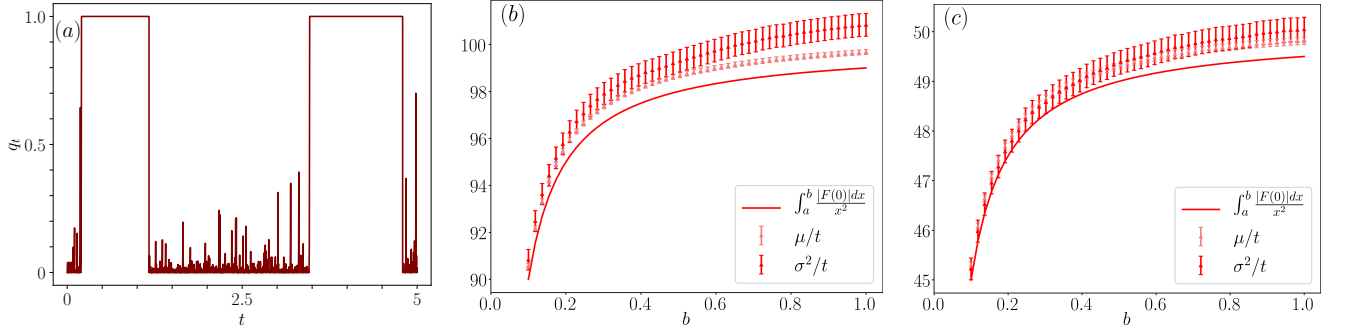


FIG. 9. (a) The typical trajectory for the general 1D PDMP (Eq. (62)) with resetting to $q^* = 0$ for $\gamma = 10^4$. The jumps between $q_t = 0$ and $q_t = 1$ are interspersed with spikes from $q_t = 0$ in the strong measurement limit. In (b) and (c), we plot the mean and variance of the distribution (conditioned on no-jumps) of the number of spikes (from $q_t = 0$) per unit time in a space-time box $(0.01, b) \times (0, t)$ against the box-edge b for (b) $F(q) = \cos(\frac{50q}{\pi})$ and (c) $F(q) = (e^{-q} - 0.5)$. Since the plots are separated by reasonable thresholds ($\sim 4\%$), this verifies the conjecture that the spiking process is Poissonian with the parameter $\int_a^b \frac{|F(0)|dx}{x^2}$. The data-points were obtained for the parameters $t = 0.1$ and $\gamma = 10^7$ by averaging over 10^5 realizations.

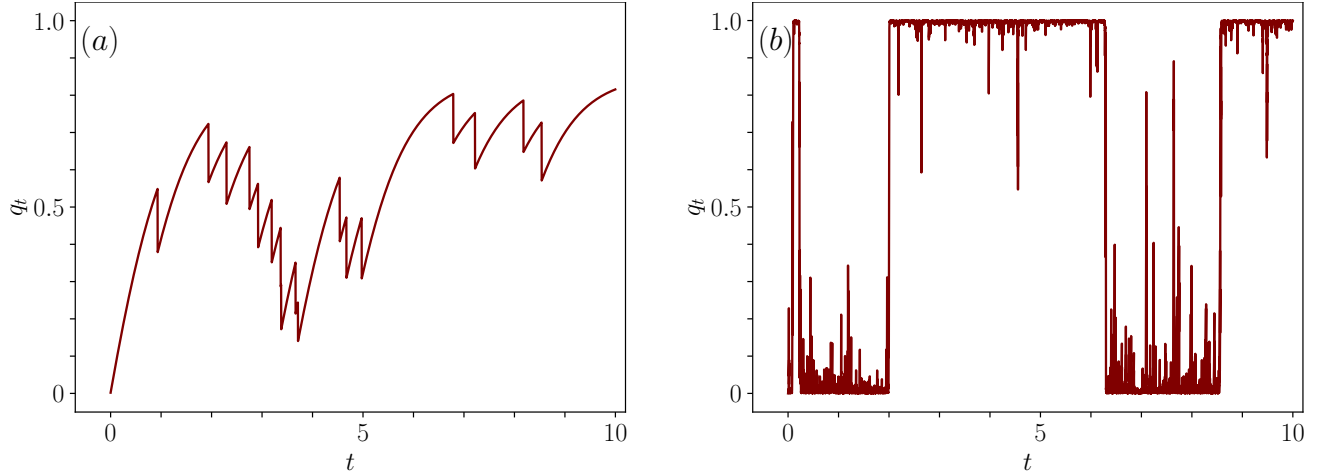


FIG. 10. Typical trajectory for (a) $\gamma = 10$ (b) $\gamma = 10^4$ for the Collapse-Thermal set-up for a general measurement operator for the parameters $|n_+|^2 = 0.2$, $|n_-|^2 = 0.4$, $W_{-,+} = 0.77$, $W_{+,-} = 0.23$. Here, (b) shows that the jumps between $q_t = 0$ and $q_t = 1$ are interspersed with spikes from both $q_t = 0$ and $q_t = 1$ in the strong measurement limit, even though the dynamics in this case does not reset to a fixed point.

dynamics to a point q^* , we require $G(q) = q^* - q$. If $q^* \neq 0$ and $q^* \neq 1$, the hypothesis Eq. (63) will only be satisfied if $H(0) = H(1) = 0$, in which case the intensity of the spiking process vanishes. Thus, to observe spikes, we take $q^* = 0$ without loss of generality. In addition, to satisfy Eq. (63), we need then to take $H(1) = 0$, so we consider $H(q) = (1 - q)\chi(q)$, where $\chi(q)$ is any finite function such that $\chi(0) \neq 0$. Then the conjecture Eq. (65) gives that $P_c[n : (s, t), a, b]$ converge at large γ to a Poisson distribution limit Eq. (65) with intensity parameter given by (one-sided spikes)

$$\lambda_{[a,b]}^{\bar{q}} = \begin{cases} \int_a^b dx \frac{|F(0)|}{x^2} & \text{if } \bar{q}|_{[s,t]} = 0, \\ 0 & \text{if } \bar{q}|_{[s,t]} = 1. \end{cases}$$

In Fig. 9, we numerically verify the conjecture by taking $\chi(q)$ to be a fourth-order polynomial with arbitrary coefficients, for two very different forms of $F(q)$:

- (i) $F(q) = \cos(\frac{50q}{\pi})$, a highly oscillatory function and
- (ii) $F(q) = (e^{-q} - 0.5)$, a strictly monotonic function.

B. Example 2 without resetting: Collapse-Thermal setup with general QND (diagonal) measurement N_1 operator

Consider the Collapse-Thermal setup for a qubit with a general diagonal measurement operator (intensity is denoted by γ and efficiency by η)

$$N_1 = \begin{pmatrix} n_+ & 0 \\ 0 & n_- \end{pmatrix}.$$

By using the computations performed in Appendix A, we easily get that, with the usual parameterization of the density matrix ρ_t^γ given in Eq. (10),

$$\begin{aligned} \dot{q}_t^\gamma &= (W_{+,-} + W_{-,+}) \left(\frac{W_{-,+}}{W_{+,-} + W_{-,+}} - q_t^\gamma \right) \\ &+ \frac{|n_+|^2 - |n_-|^2}{(|n_+|^2 - |n_-|^2)q_t^\gamma + |n_-|^2} (1 - q_t^\gamma) q_t^\gamma \left(\dot{\mathcal{N}}_t^\gamma - \mathbb{E} \left(\dot{\mathcal{N}}_t^\gamma | q_t^\gamma \right) \right), \end{aligned} \quad (68)$$

with $d\mathcal{N}_t^\gamma d\mathcal{N}_t^\gamma = d\mathcal{N}_t^\gamma$

$$\mathbb{E} (d\mathcal{N}_t^\gamma | q_t^\gamma) = \gamma \eta \left[(|n_+|^2 - |n_-|^2) q_t^\gamma + |n_-|^2 \right]. \quad (69)$$

Observe that Eq. (68) takes the form of Eq. (62) with

$$\begin{aligned} F(q) &= (W_{+,-} + W_{-,+}) \left(\frac{W_{-,+}}{W_{+,-} + W_{-,+}} - q \right), \\ G(q) &= \frac{|n_+|^2 - |n_-|^2}{(|n_+|^2 - |n_-|^2)q + |n_-|^2} (1 - q)q, \\ H(q) &= \eta \left[(|n_+|^2 - |n_-|^2)q + |n_-|^2 \right]. \end{aligned} \quad (70)$$

In particular, for the model considered in Eq. (20), i.e. $n_+ = 0$, $n_- = 1$ (resetting dynamics), we have that our conjecture is satisfied with spikes only from 0 and spikes statistics described by the spike process \mathbb{Q} defined in Eq. (64).

But our conjecture claims that, moreover, in general (even without resetting dynamics), there are spikes starting from 0 and from 1. This is the case if $F(0)H(0) = \eta W_{-,+} |n_-|^2 \neq 0$ (spikes from 0 to 1) and $F(1)H(1) = \eta W_{+,-} |n_+|^2 \neq 0$ (spikes from 1 to 0). This is confirmed by numerical simulations (see Fig. 10).

Observe moreover that if we consider the measurement operator $N_1 = \sigma_z$ (hence $|n_-|^2 = |n_+|^2$), as it was considered in the Gaussian case [48, 51, 52, 54], we get a purely deterministic equation without jumps or spikes. This is very different from the studies cited previously in the Gaussian noise context.

C. Example 3 with resetting: Collapse-Measurement setup for QND resetting $N_1 = |- \rangle \langle - |$ but general N_2 operator

To generalize the Collapse-Measurement setup given by equation Eq. (23), we can substitute the damping-spontaneous emission operator N_2 , defined in Eq. (21), by a general (not necessarily diagonal) measurement operator N_2 (in order to break the QND assumption). Then, we can check that, generically, the equation for q^γ is not autonomous. More exactly, the non-commutativity of N_2 w.r.t. N_1 (to break the QND assumption) and the fact that q^γ has an autonomous evolution, are equivalent to taking N_2 in the form

$$N_2 = \begin{pmatrix} 0 & a \\ b & 0 \end{pmatrix}, \quad ab \neq 0. \quad (71)$$

The requirement that q^γ has an autonomous evolution seems to be a necessary condition to adapt our analytical proof (technical assumption).

Observe, however that, even in this case, the Collapse-Measurement setup does not fall directly in our conjecture case Eq. (62) because we have then two Poisson noises involved (but the second one is weaker than the first one since γ_2 is of order one while γ_1 is very large). More precisely, the equation for q^γ is given by (Appendix B)

$$\dot{q}_t^\gamma = F(q_t^\gamma) + G_1(q_t^\gamma) \left(\dot{\mathcal{N}}_t^{1,\gamma} - \gamma_1 H_1(q_t^\gamma) \right) + G_2(q_t^\gamma) \dot{\mathcal{N}}_t^{2,\gamma}, \quad (72)$$

with

$$\begin{aligned} F(q) &= \gamma_2 \left\{ |a|^2 - (|a|^2 + |b|^2)q \right\} \{1 - \eta_2 G_2(q)\}, \\ G_2(q) &= \frac{|a|^2(1-q)}{|a|^2(1-q) + |b|^2q} - q, \\ H_2(q) &= \eta_2 (|a|^2(1-q) + |b|^2q), \\ G_1(q) &= -q, \\ H_1(q) &= \eta_1(1-q), \end{aligned}$$

and the Poisson noises satisfy

$$\begin{aligned} \mathbb{E} \left(d\mathcal{N}_t^{k,\gamma} | q_t^\gamma \right) &= H_k(q_t^\gamma) dt, \\ d\mathcal{N}_t^{k,\gamma} d\mathcal{N}_t^{\ell,\gamma} &= \delta_{k\ell} d\mathcal{N}_t^{k,\gamma}. \end{aligned}$$

Hence, a stronger conjecture of the one above is that, if we have an evolution equation given by Eq. (72) with hypothesis Eq. (63), then in the large limit $\gamma_1 \rightarrow \infty$, γ_2 of order 1, the graph of q^γ should converge to a spiking process \mathbb{Q} , given by Eq. (64) with H replaced there by the dominant term H_1 . Since $F(1)H_1(1) = 0$, we expect only to have no spikes from 1 (apart from the degenerate case $\gamma_2 |a|^2(1 - \eta_2) = 0$, see below, we will always have spikes from 0).

In the present paper, we considered only N_2 equal to the damping-spontaneous emission operator appearing in Eq. (21), which corresponds to the case $a = 1$ and $b = 0$, and then the previous conjecture about the spike statistics is in agreement with the third relation in Eq. (25) because $F(0) = \gamma_2(1 - \eta_2)$. Another standard rank one choice is to take N_2 equal to the spontaneous absorption operator given by

$$N_2 = \begin{pmatrix} 0 & 0 \\ 1 & 0 \end{pmatrix} = |- \rangle \langle + |.$$

In the latter case ($a = 0, b = 1$) we have then a competition between a strong resetting dynamics and a weak resetting dynamics towards the same $|- \rangle \langle - |$. Our conjecture implies thus that in this case, we do not have spikes but only jumps.

VII. CONCLUSION

In this work, we discussed finite-dimensional quantum trajectories driven by Poissonian noises, see Eq. (1), in a strong measurement limit and focused our studies to a qubit system in three different setups where the Quantum-Non-Demolition condition for the strong measurement is broken by a unitary evolution, a thermal bath or a second measurement, see Sec.III. Our analytical studies of Sec. V establish that the quantum trajectory investigated behaves like a pure jump Markov process in the strong measurement limit. However, this rough picture can be refined and it appears in fact that this quantum jump Markov process is in fact decorated by vertical lines (called spikes). The first analytical description of spikes was done recently by Bauer-Bernard-Tilloy [48, 51, 52], and motivated some others works [53, 54], but in the context of quantum trajectories of a qubit driven by a Gaussian noise.

This paper is therefore the first to investigate this question for quantum trajectories driven by Poissonian noises.

Observe that in all the setups we studied analytically, we observe a kind of universal law for the distribution of spikes, see Eq. (24), valid for Gaussian or Poissonian noises. Numerical experiments confirm our analytical results.

A fundamental property used to perform our analytical investigation in Sec. V is that the evolution of the quantum trajectory can be reduced to the evolution of a one-dimensional piecewise Markovian deterministic process with resetting. Hence, apart from its interest in this quantum framework, this problem could be subject of investigation in the resetting literature. Moreover, it seems that the existence of spikes is more generic and they can appear in other piecewise Markovian deterministic processes which do not have a resetting property, see e.g. Fig. 10. In Sec. VI we provide a general conjecture for the distribution of the spikes in a general one-dimensional framework.

Quantum trajectories are now routinely realized in experiments [25–30, 80], but spikes have not yet been seen. Thus, a few remarks on the experimental detection of spikes are in order. Strictly speaking, spikes emerge in the $\gamma \rightarrow \infty$ limit, but their statistical properties can be observed for large but finite γ , as evidenced by our numerical results. We note that in experiments, we have access to the click sequence records, and it is in principle possible to do quantum state tomography for the state conditioned on no clicks. These are sufficient to reconstruct the entire quantum trajectory from which the spike statistics can be obtained. Experimental platforms like superconducting qubits [81, 82] have demonstrated highly efficient detection of clicks and are promising avenues for the detection of spikes in the near future.

ACKNOWLEDGMENTS

We thank Michel Bauer, Reda Chhaibi, Clement Pellegrini for useful discussions. This work was supported by the projects RETENU ANR-20-CE40 of the French National Research Agency (ANR). AS and AD acknowledge financial support of the Department of Atomic Energy, Government of India, under Project Identification No. RTI 4001. AK acknowledges financial support for project NDFluc U-AGR-7239-00-C from the Luxembourg National Research Fund, Fonds National de la Recherche. AD acknowledges the J.C. Bose Fellowship (JCB/2022/000014) of the Science and Engineering Research Board of the Department of Science and Technology, Government of India. AD and AK thanks Laboratoire J A Dieudonné and INPHYNI, Nice for supporting a visit which initiated this project. AD thanks the National Research University Higher School of Economics, Moscow for supporting a visit. RC thanks ICTS-TIFR for supporting a visit for the completion of the project.

-
- [1] D. Bohm and J. Bub, A proposed solution of the measurement problem in quantum mechanics by a hidden variable theory, *Rev. Mod. Phys.* **38**, 453 (1966).
- [2] P. Pearle, Reduction of the state vector by a nonlinear Schrödinger equation, *Phys. Rev. D* (3) **13**, 857 (1976).
- [3] P. Pearle, Stochastic dynamical reduction theories and superluminal communication, *Phys. Rev. D* (3) **33**, 2240 (1986).
- [4] L. Diósi, Stochastic pure state representation for open quantum systems, *Phys. Lett. A* **114**, 451 (1986).
- [5] N. Gisin, Quantum measurements and stochastic processes, *Phys. Rev. Lett.* **52**, 1657 (1984).
- [6] A. Barchielli, Measurement theory and stochastic differential equations in quantum mechanics, *Phys. Rev. A* (3) **34**, 1642 (1986).
- [7] R. Alicki and M. Fannes, On dilating quantum dynamical semigroups with classical Brownian motion, *Lett. Math. Phys.* **11**, 259 (1986).
- [8] L. Diósi, Continuous quantum measurement and Itô formalism, *Phys. Lett. A* **129**, 419 (1988).
- [9] V. P. Belavkin, A new wave equation for a continuous nondemolition measurement, *Phys. Lett. A* **140**, 355 (1989).
- [10] V. P. Belavkin, A posteriori Schrödinger equation for continuous nondemolition measurement, *J. Math. Phys.* **31**, 2930 (1990).
- [11] A. Barchielli and V. P. Belavkin, Measurements continuous in time and a posteriori states in quantum mechanics, *J. Phys. A* **24**, 1495 (1991).
- [12] V. P. Belavkin, Quantum continual measurements and a posteriori collapse on CCR, *Comm. Math. Phys.* **146**, 611 (1992).
- [13] P. a. Staszewski, Viacheslav Pavlovich Belavkin, 1946–2012: In memory of Professor V. P. Belavkin, *Open Syst. Inf. Dyn.* **20**, 1377001, 2 (2013).
- [14] M. Holland, S. Marksteiner, P. Marte, and P. Zoller, Measurement induced localization from spontaneous decay, *Phys. Rev. Lett.* **76**, 3683 (1996).
- [15] C. W. Gardiner, A. S. Parkins, and P. Zoller, Wavefunction quantum stochastic differential equations and quantum-jump simulation methods, *Phys. Rev. A* (3) **46**, 4363 (1992).
- [16] J. Dalibard, Y. Castin, and K. Mølmer, Wave-function approach to dissipative processes in quantum optics, *Phys. Rev. Lett.* **68**, 580 (1992).
- [17] H. M. Wiseman and G. J. Milburn, Quantum theory of field-quadrature measurements, *Phys. Rev. A* **47**, 642 (1993).
- [18] B. M. Garraway and P. L. Knight, Evolution of quantum superpositions in open environments: Quantum trajectories, jumps, and localization in phase space, *Phys. Rev. A* **50**, 2548 (1994).
- [19] C. W. Gardiner and P. Zoller, *Quantum noise*, 3rd ed., Springer Series in Synergetics (Springer-Verlag, Berlin, 2004) pp. xxii+449, a handbook of Markovian and non-Markovian quantum stochastic methods with applications to quantum optics.
- [20] H. M. Wiseman and G. J. Milburn, *Quantum measurement and control* (Cambridge University Press, Cambridge, 2010) pp. xvi+460.
- [21] S. Haroche and J.-M. Raimond, *Exploring the quantum*, Oxford Graduate Texts (Oxford University Press, Oxford, 2006) pp. x+605, atoms, cavities and photons.
- [22] H.-P. Breuer and F. Petruccione, *The theory of open quantum systems* (Oxford University Press, New York, 2002) pp. xxii+625.
- [23] H. Carmichael, *An open systems approach to quantum optics: lectures presented at the Université Libre de Bruxelles, October 28 to November 4, 1991*, Vol. 18 (Springer Science & Business Media, 2009).
- [24] K. Jacobs, *Quantum measurement theory and its applications* (Cambridge University Press, 2014).
- [25] C. Guerlin, J. Bernu, S. Deleglise, C. Sayrin, S. Gleyzes, S. Kuhr, M. Brune, J.-M. Raimond, and S. Haroche, Progressive field-state collapse and quantum non-demolition photon counting, *Nature* **448**, 889 (2007).
- [26] S. Gleyzes, S. Kuhr, C. Guerlin, J. Bernu, S. Deleglise, U. Busk Hoff, M. Brune, J.-M. Raimond, and S. Haroche, Quantum jumps of light recording the birth and death of a photon in a cavity, *Nature* **446**, 297 (2007).
- [27] C. Sayrin, I. Dotsenko, X. Zhou, B. Peaudecerf, T. Rybarczyk, S. Gleyzes, P. Rouchon, M. Mirrahimi, H. Amini, M. Brune, *et al.*, Real-time quantum feedback prepares and stabilizes photon number states, *Nature* **477**, 73 (2011).
- [28] K. Murch, S. Weber, K. Beck, E. Ginossar, and I. Siddiqi, Reduction of the radiative decay of atomic coherence in squeezed vacuum, *Nature* **499**, 62 (2013).
- [29] K. W. Murch, S. Weber, C. Macklin, and I. Siddiqi, Observing single quantum trajectories of a superconducting quantum bit, *Nature* **502**, 211 (2013).
- [30] S. Weber, A. Chantasri, J. Dressel, A. N. Jordan, K. W. Murch, and I. Siddiqi, Mapping the optimal route between two quantum states, *Nature* **511**, 570 (2014).
- [31] S. L. Adler, D. C. Brody, T. A. Brun, and L. P. Hughston, Martingale models for quantum state reduction, *J. Phys. A* **34**, 8795 (2001).
- [32] R. van Handel, J. K. Stockton, and H. Mabuchi, Feedback control of quantum state reduction, *IEEE Trans. Automat. Control* **50**, 768 (2005).
- [33] H. Maassen and B. Kümmerer, Purification of quantum trajectories, in *Dynamics & stochasticity*, IMS Lecture Notes Monogr. Ser., Vol. 48 (Inst. Math. Statist., Beachwood, OH, 2006) pp. 252–261.
- [34] M. Bauer and D. Bernard, Convergence of repeated quantum nondemolition measurements and wave-function collapse, *Phys. Rev. A* **84**, 044103 (2011).
- [35] T. Benoist and C. Pellegrini, Large time behavior and convergence rate for quantum filters under standard non demolition conditions, *Comm. Math. Phys.* **331**, 703 (2014).
- [36] N. Bohr, I. on the constitution of atoms and molecules, *The London, Edinburgh, and Dublin Philosophical Magazine and Journal of Science* **26**, 1 (1913).
- [37] W. Nagourney, J. Sandberg, and H. Dehmelt, Shelved optical electron amplifier: Observation of quantum jumps, *Phys. Rev. Lett.* **56**, 2797 (1986).
- [38] T. Sauter, W. Neuhauser, R. Blatt, and P. E. Toschek, Observation of quantum jumps, *Phys. Rev. Lett.* **57**, 1696 (1986).

- [39] M. Bauer, D. Bernard, and A. Tilloy, Computing the rates of measurement-induced quantum jumps, *J. Phys. A* **48**, 25FT02, 15 (2015).
- [40] T. Benoist, C. Bernardin, R. Chetrite, R. Chhaibi, J. Najnudel, and C. Pellegrini, Emergence of jumps in quantum trajectories via homogenization, *Comm. Math. Phys.* **387**, 1821 (2021).
- [41] M. Ballesteros, N. Crawford, M. Fraas, J. Fröhlich, and B. Schubnel, Perturbation theory for weak measurements in quantum mechanics, systems with finite-dimensional state space, *Ann. Henri Poincaré* **20**, 299 (2019).
- [42] A. Degasperis, L. Fonda, and G. C. Ghirardi, Does the Lifetime of an Unstable System Depend on the Measuring Apparatus?, *Nuovo Cim. A* **21**, 471 (1973).
- [43] B. Misra and E. C. G. Sudarshan, The Zeno's paradox in quantum theory, *J. Mathematical Phys.* **18**, 756 (1977).
- [44] A. Peres, Measurement of time by quantum clocks, *Amer. J. Phys.* **48**, 552 (1980).
- [45] W. M. Itano, D. J. Heinzen, J. J. Bollinger, and D. J. Wineland, Quantum zeno effect, *Phys. Rev. A* **41**, 2295 (1990).
- [46] C. Teuscher, Turing's connectionism, in *Alan Turing: life and legacy of a great thinker* (Springer, Berlin, 2004) pp. 499–529.
- [47] D. Layden, E. Martín-Martínez, and A. Kempf, Perfect zeno-like effect through imperfect measurements at a finite frequency, *Phys. Rev. A* **91**, 022106 (2015).
- [48] A. Tilloy, M. Bauer, and D. Bernard, Spikes in quantum trajectories, *Phys. Rev. A* **92**, 052111 (2015).
- [49] N. Gisin and I. C. Percival, The quantum-state diffusion model applied to open systems, *J. Phys. A* **25**, 5677 (1992).
- [50] H. Mabuchi and H. M. Wiseman, Retroactive quantum jumps in a strongly coupled atom-field system, *Phys. Rev. Lett.* **81**, 4620 (1998).
- [51] M. Bauer, D. Bernard, and A. Tilloy, Zooming in on quantum trajectories, *J. Phys. A* **49**, 10LT01, 9 (2016).
- [52] M. Bauer and D. Bernard, Stochastic spikes and strong noise limits of stochastic differential equations, *Ann. Henri Poincaré* **19**, 653 (2018).
- [53] M. Kolb and M. Liesenfeld, Stochastic spikes and Poisson approximation of one-dimensional stochastic differential equations with applications to continuously measured quantum systems, *Ann. Henri Poincaré* **20**, 1753 (2019).
- [54] C. Bernardin, R. Chetrite, R. Chhaibi, J. Najnudel, and C. Pellegrini, Spiking and collapsing in large noise limits of sdes, *The Annals of Applied Probability* **33**, 417 (2023).
- [55] A. Tilloy, Continuous collapse models on finite dimensional hilbert spaces, in *Do Wave Functions Jump?* (Springer International Publishing, 2020) pp. 167–188.
- [56] M. R. Evans and S. N. Majumdar, Diffusion with stochastic resetting, *Phys. Rev. Lett.* **106**, 160601 (2011).
- [57] M. R. Evans and S. N. Majumdar, Diffusion with optimal resetting, *Journal of Physics A: Mathematical and Theoretical* **44**, 435001 (2011).
- [58] M. R. Evans, S. N. Majumdar, and G. Schehr, Stochastic resetting and applications, *Journal of Physics A: Mathematical and Theoretical* **53**, 193001 (2020).
- [59] A. Pal, A. Kundu, and M. R. Evans, Diffusion under time-dependent resetting, *J. Phys. A* **49**, 225001, 19 (2016).
- [60] V. Gorini, A. Kossakowski, and E. C. G. Sudarshan, Completely positive dynamical semigroups of N -level systems, *J. Mathematical Phys.* **17**, 821 (1976).
- [61] G. Lindblad, On the generators of quantum dynamical semigroups, *Comm. Math. Phys.* **48**, 119 (1976).
- [62] Completely positive trace preserving map from $M_d(\mathbb{C})$ to $M_d(\mathbb{C})$.
- [63] C. Pellegrini, Existence, uniqueness and approximation of a stochastic Schrödinger equation: the diffusive case, *Ann. Probab.* **36**, 2332 (2008).
- [64] V. B. Braginskii and Y. I. Vorontsov, Quantum-mechanical limitations in macroscopic experiments and modern experimental technique, *Soviet Physics Uspekhi* **17**, 644 (1975).
- [65] K. S. Thorne, R. W. Drever, C. M. Caves, M. Zimmermann, and V. D. Sandberg, Quantum nondemolition measurements of harmonic oscillators, *Physical Review Letters* **40**, 667 (1978).
- [66] W. G. Unruh, Quantum nondemolition, in *Gravitational radiation, collapsed objects and exact solutions (Proc. Einstein Centenary Summer School, Perth, 1979)*, *Lecture Notes in Phys.*, Vol. 124 (Springer, Berlin-New York, 1980) pp. 385–426.
- [67] V. B. Braginsky, Y. I. Vorontsov, and K. S. Thorne, Quantum nondemolition measurements, *Science* **209**, 547 (1980), <https://www.science.org/doi/pdf/10.1126/science.209.4456.547>.
- [68] C. M. Caves, K. S. Thorne, R. W. Drever, V. D. Sandberg, and M. Zimmermann, On the measurement of a weak classical force coupled to a quantum-mechanical oscillator. i. issues of principle, *Reviews of Modern Physics* **52**, 341 (1980).
- [69] G. J. Milburn and D. F. Walls, Quantum nondemolition measurements via quadratic coupling, *Phys. Rev. A* **28**, 2065 (1983).
- [70] W. H. Zurek, Pointer basis of quantum apparatus: into what mixture does the wave packet collapse?, *Phys. Rev. D* (3) **24**, 1516 (1981).
- [71] É. Roldán, I. Neri, R. Chetrite, S. Gupta, S. Pigolotti, F. Jülicher, and K. Sekimoto, Martingales for physicists: a treatise on stochastic thermodynamics and beyond, *Advances in Physics* **72**, 1 (2023).
- [72] R. Feynman, R. Leighton, and M. Sands, *The Feynman Lectures on Physics*, Vol. II (Addison-Wesley, Boston, 1964) Chap. 35.
- [73] M. Le Bellac, *Quantum Physics*, edited by P. d. Forcrand-Millard (Cambridge University Press, 2006).
- [74] This parameterisation is quite unusual but it is convenient for our purpose.
- [75] K. Snizhko, P. Kumar, and A. Romito, Quantum zeno effect appears in stages, *Phys. Rev. Res.* **2**, 033512 (2020).
- [76] V. Dubey, R. Chetrite, and A. Dhar, Quantum resetting in continuous measurement induced dynamics of a qubit, *J. Phys. A* **56**, Paper No. 154001, 26 (2023).
- [77] E. B. Davies, *Quantum theory of open systems* (Academic Press [Harcourt Brace Jovanovich, Publishers], London-New York, 1976) pp. x+171.
- [78] The fact that the state space is $\{0, \pi\}$ and not $\{0, 1\}$ is due to the change of variable done in Eq. (15).
- [79] V. Dubey, R. Chetrite, and A. Dhar, Quantum resetting in continuous measurement induced dynamics of a qubit, *Journal of Physics A: Mathematical and Theoretical* **56**, 154001 (2023).

- [80] G. de Lange, D. Ristè, M. J. Tiggelman, C. Eichler, L. Tornberg, G. Johansson, A. Wallraff, R. N. Schouten, and L. DiCarlo, Reversing quantum trajectories with analog feedback, *Phys. Rev. Lett.* **112**, 080501 (2014).
- [81] Z. K. Mineev, S. O. Mundhada, S. Shankar, P. Reinhold, R. Gutiérrez-Jáuregui, R. J. Schoelkopf, M. Mirrahimi, H. J. Carmichael, and M. H. Devoret, To catch and reverse a quantum jump mid-flight, *Nature* **570**, 200 (2019).
- [82] R. Vijay, D. H. Slichter, and I. Siddiqi, Observation of quantum jumps in a superconducting artificial atom, *Phys. Rev. Lett.* **106**, 110502 (2011).
- [83] D. Applebaum, Levy processes and stochastic calculus, *Cambridge Studies in Advanced Mathematics* **116** (2009).
- [84] P. Tankov, *Financial modelling with jump processes* (Chapman and Hall/CRC, 2003).

Appendix A: Measurement part of the SME Eq. (1) for qubit with a general diagonal measurement operator

We perform here computations in a more general framework where the measurement operator N is still diagonal

$$N = \begin{pmatrix} n_+ & 0 \\ 0 & n_- \end{pmatrix}$$

but not necessary of rank one like in Eq. (7).

We consider hence only the dynamics generated by the measurement operator N with intensity $\gamma > 0$ and efficiency η :

$$\dot{\rho}_t^\gamma = \gamma L_N [\rho_t^\gamma] + M_N [\rho_t^\gamma] \left[\dot{\mathcal{N}}_t^\gamma - \gamma \eta \text{Tr} (N \rho_t^\gamma N^\dagger) \right] \quad (\text{A1})$$

with the noise \mathcal{N}_t^γ satisfying $d\mathcal{N}_t^\gamma \in \{0, 1\}$, $d\mathcal{N}_t^\gamma d\mathcal{N}_t^\gamma = d\mathcal{N}_t^\gamma$, and

$$\mathbb{E} (d\mathcal{N}_t^\gamma | \rho_t^\gamma) = \eta \gamma \text{Tr} (N \rho_t^\gamma N^\dagger) dt. \quad (\text{A2})$$

We use the usual parameterisation of the density matrix ρ_t^γ given in Eq. (10). Then Eq. (A1) takes the form of a three dimensional (because even if q^γ is real, p^γ is complex) piecewise deterministic Markov process

$$\begin{aligned} \dot{q}_t^\gamma &= \alpha(q_t^\gamma) \left(\dot{\mathcal{N}}_t^\gamma - \mathbb{E} \left(\dot{\mathcal{N}}_t^\gamma | q_t^\gamma \right) \right) \\ \dot{p}_t^\gamma &= -\frac{\gamma}{2} (|n_+|^2 + |n_-|^2 - 2\bar{n}_+ n_-) p_t^\gamma \\ &\quad + \beta(q_t^\gamma) p_t^\gamma \left(\dot{\mathcal{N}}_t^\gamma - \mathbb{E} \left(\dot{\mathcal{N}}_t^\gamma | q_t^\gamma \right) \right) \end{aligned} \quad (\text{A3})$$

with

$$\begin{aligned} \alpha(q_t^\gamma) &= \frac{(|n_+|^2 - |n_-|^2) q_t^\gamma (1 - q_t^\gamma)}{(|n_+|^2 - |n_-|^2) q_t^\gamma + |n_-|^2}, \\ \beta(q_t^\gamma) &= \frac{\bar{n}_+ n_-}{(|n_+|^2 - |n_-|^2) q_t^\gamma + |n_-|^2} - 1, \end{aligned} \quad (\text{A4})$$

and

$$\begin{aligned} \mathbb{E} (d\mathcal{N}_t^\gamma | q_t^\gamma) &= \gamma \eta \{ (|n_+|^2 - |n_-|^2) q_t^\gamma + |n_-|^2 \} dt, \\ d\mathcal{N}_t^\gamma d\mathcal{N}_t^\gamma &= d\mathcal{N}_t^\gamma. \end{aligned}$$

Observe that the diagonal dynamics is autonomous.

1. Resetting dynamics or not

The transition rate of the Poisson noise in Eq. (A1) are given by

$$\begin{aligned} W((q, p) \rightarrow, (q', p')) &= \gamma \eta ((|n_+|^2 - |n_-|^2) q + |n_-|^2) \\ &\quad \times \delta \left(q' - \frac{|n_+|^2 q}{(|n_+|^2 - |n_-|^2) q + |n_-|^2} \right) \\ &\quad \times \delta \left(p' - \frac{\bar{n}_+ n_- p}{(|n_+|^2 - |n_-|^2) q + |n_-|^2} \right). \end{aligned} \quad (\text{A5})$$

Observe that these jumps correspond to a resetting dynamics towards a point if and only if for any q, p we have that

$$\frac{|n_+|^2 q}{(|n_+|^2 - |n_-|^2)q + |n_-|^2} = k_1, \quad \frac{\overline{n_+ n_-} p}{(|n_+|^2 - |n_-|^2)q + |n_-|^2} = k_2,$$

where k_1, k_2 are two arbitrary fixed constants, i.e. independent of q, p . We show easily that there is only two possibilities to have that. The first one is that

$$k_1 = 0 = k_2, \quad n_+ = 0, \quad \text{i.e.} \quad N = \begin{pmatrix} 0 & 0 \\ 0 & 1 \end{pmatrix} = N_1$$

and the second one is

$$k_1 = 1, \quad k_2 = 0, \quad n_- = 0, \quad \text{i.e.} \quad N = \begin{pmatrix} 1 & 0 \\ 0 & 0 \end{pmatrix}.$$

2. Proof of Eq. (A3)

The proof is based on elementary algebraic computations. We have that the Lindbladian term is given by

$$\begin{aligned} L_N [\rho_t^\gamma] &= N \rho_t^\gamma N^\dagger - \frac{1}{2} N^\dagger N \rho_t^\gamma - \frac{1}{2} \rho_t^\gamma N^\dagger N \\ &= \begin{pmatrix} 0 & -\frac{|n_+|^2 + |n_-|^2 - 2n_+ \overline{n_-}}{2} \overline{p_t^\gamma} \\ -\frac{|n_+|^2 + |n_-|^2 - 2\overline{n_+} n_-}{2} p_t^\gamma & 0 \end{pmatrix}. \end{aligned}$$

The "stochastic innovation" term is given by

$$M_N [\rho_t^\gamma] = \frac{N \rho_t^\gamma N^\dagger}{\text{Tr}(N \rho_t^\gamma N^\dagger)} - \rho_t^\gamma = \begin{pmatrix} \alpha(q_t^\gamma) & \overline{\beta}(q_t^\gamma) \overline{p_t^\gamma} \\ \beta(q_t^\gamma) p_t^\gamma & -\alpha(q_t^\gamma) \end{pmatrix}$$

where α, β have been defined in Eq. (A4).

Appendix B: Proof of Eq. (72) and of Eq. (23)

We consider Eq. (71)

$$N_2 = \begin{pmatrix} 0 & a \\ b & 0 \end{pmatrix}, \quad ab \neq 0. \quad (\text{B1})$$

Observe that

$$\begin{aligned} L_{N_2} [\rho_t^\gamma] &= N_2 \rho_t^\gamma N_2^\dagger - \frac{1}{2} N_2^\dagger N_2 \rho_t^\gamma - \frac{1}{2} \rho_t^\gamma N_2^\dagger N_2 \\ &= \begin{pmatrix} |a|^2 (1 - q_t^\gamma) - |b|^2 q_t^\gamma & a \overline{b} p_t^\gamma - \frac{|b|^2 + |a|^2}{2} \overline{p_t^\gamma} \\ \overline{a} b p_t^\gamma - \frac{|b|^2 + |a|^2}{2} p_t^\gamma & |b|^2 q_t^\gamma - |a|^2 (1 - q_t^\gamma) \end{pmatrix} \end{aligned}$$

and

$$\begin{aligned} M_{N_2} [\rho_t^\gamma] &= \frac{N_2 \rho_t^\gamma N_2^\dagger}{\text{Tr}(N_2 \rho_t^\gamma N_2^\dagger)} - \rho_t^\gamma \\ &= \begin{pmatrix} \frac{|a|^2 (1 - q_t^\gamma)}{|a|^2 (1 - q_t^\gamma) + |b|^2 q_t^\gamma} - q_t^\gamma & \frac{a \overline{b} p_t^\gamma}{|a|^2 (1 - q_t^\gamma) + |b|^2 q_t^\gamma} - \overline{p_t^\gamma} \\ \frac{\overline{a} b p_t^\gamma}{|a|^2 (1 - q_t^\gamma) + |b|^2 q_t^\gamma} - p_t^\gamma & \frac{|b|^2 q_t^\gamma}{|a|^2 (1 - q_t^\gamma) + |b|^2 q_t^\gamma} - 1 + q_t^\gamma \end{pmatrix}. \end{aligned}$$

Then, with the equation Eq. (11) for the N_1 -measurement part, we obtain finally the equation Eq. (72). In the particular case of spontaneous emission Eq. (21):

$$N_2 = \begin{pmatrix} 0 & 1 \\ 0 & 0 \end{pmatrix} = |+\rangle\langle -|, \quad (\text{B2})$$

the equation Eq. (11) becomes the equation Eq. (23).

Appendix C: Proof of Eq. (17)

We consider the SME Eq. (1) in the Collapse-Unitary setup Eq. (12) (see Eq. (14) with the usual parameterisation of the density matrix ρ_t^γ given in Eq. (10)).

To simplify notation, we denote now γ_1 by γ by η , $\mathcal{N}_t^{\gamma,1}$ by \mathcal{N}_t^γ .

Parameterising now the density matrix in Bloch coordinates (Eq. (15)), we prove below that

$$\begin{aligned} \frac{d}{dt} (r_t^\gamma)^2 &= \gamma (\eta - 1) 2(1 - q_t^\gamma) ((r_t^\gamma)^2 + 2q_t^\gamma - 1) \\ &\quad + (1 - (r_t^\gamma)^2) [\gamma (2q_t^\gamma - 1) + \mathcal{N}_t^\gamma]. \end{aligned} \quad (\text{C1})$$

Then, we can conclude that if the measurement is totally efficient, i.e. $\eta = 1$, then the Bloch sphere $r = 1$ (pure states) is stable under the dynamics. We will restrict us to this case now, i.e. pure state dynamics ($r_t^\gamma = 1$) and totally efficient $\eta = 1$.

The Bloch sphere of pure states can be parameterised with the angles $\theta_t^\gamma \in (-\pi, \pi]$, $\varphi_t^\gamma \in [0, \pi]$, see Eq. (15):

$$q_t^\gamma = \cos^2\left(\frac{\theta_t^\gamma}{2}\right), \quad p_t^\gamma = \frac{(\sin \theta_t^\gamma)}{2} e^{i\varphi_t^\gamma}. \quad (\text{C2})$$

We then look for an SDE for $(\theta_t^\gamma, \varphi_t^\gamma)$ which gives a solution to the sde Eq. (14). We claim that if $(\theta_t^\gamma, \varphi_t^\gamma)$ satisfies the sde

$$\begin{cases} \dot{\theta}_t^\gamma = (-2k_\gamma \sin(\varphi_t^\gamma) - \frac{\gamma}{2} \sin(\theta_t^\gamma)) + (\pi - \theta_t^\gamma) \mathcal{N}_t^\gamma, \\ \dot{\varphi}_t^\gamma = -2k_\gamma \frac{\cos(\theta_t^\gamma)}{\sin(\theta_t^\gamma)} \cos(\varphi_t^\gamma) \end{cases} \quad (\text{C3})$$

with

$$\mathbb{E}(d\mathcal{N}_t^\gamma | \theta_t^\gamma) = \gamma \left(\sin \frac{\theta_t^\gamma}{2}\right)^2 dt, \quad d\mathcal{N}_t^\gamma d\mathcal{N}_t^\gamma = d\mathcal{N}_t^\gamma,$$

then (q_t^γ, p_t^γ) defined through Eq. (C2) satisfied the sde Eq. (14).

To prove this claim, it is sufficient to apply the Ito-jump stochastic calculus [83, 84].

In fact we see that the sde Eq. (C3) is not well defined when $\theta_t^\gamma = \pi$, so that some extra boundary conditions should be added to defined it correctly. This is due to the fact that the change of variable Eq. (C2) is not smooth. However, in the particular case we consider, where $\varphi_t^\gamma = \pi/2$, we can disregard this technical issue.

1. Proof of Eq. (C1)

We have $(r_t^\gamma)^2 = (2q_t^\gamma - 1)^2 + 4p_t^\gamma \bar{p}_t^\gamma$ and then with Ito-jump stochastic calculus

$$\begin{aligned} d(r_t^\gamma)^2 &= d \left[(2q_t^\gamma - 1)^2 + 4p_t^\gamma \bar{p}_t^\gamma \right] \\ &= 4(2q_t^\gamma - 1) (dq_t^\gamma)_c + 4(dp_t^\gamma)_c \bar{p}_t^\gamma + 4p_t^\gamma (d\bar{p}_t^\gamma)_c \\ &\quad + (2(q_t^\gamma - q_t^\gamma d\mathcal{N}_t^\gamma) - 1)^2 - (2q_t^\gamma - 1)^2 \\ &\quad + 4((p_t^\gamma - q_t^\gamma d\mathcal{N}_t^\gamma)(\bar{p}_t^\gamma - q_t^\gamma d\mathcal{N}_t^\gamma) - p_t^\gamma \bar{p}_t^\gamma) \end{aligned}$$

with

$$\begin{cases} (dq_t^\gamma)_c = ik_\gamma (p_t^\gamma - \bar{p}_t^\gamma) + \gamma \eta q_t^\gamma (1 - q_t^\gamma) , \\ (dp_t^\gamma)_c = -ik_\gamma (2q_t^\gamma - 1) - \frac{\gamma}{2} p_t^\gamma + \gamma \eta \bar{p}_t^\gamma (1 - q_t^\gamma) , \\ (d\bar{p}_t^\gamma)_c = +ik_\gamma (2q_t^\gamma - 1) - \frac{\gamma}{2} \bar{p}_t^\gamma + \gamma \eta p_t^\gamma (1 - q_t^\gamma) . \end{cases}$$

We have

$$\begin{aligned} d(r_t^\gamma)^2 &= d \left((2q_t^\gamma - 1)^2 + 4p_t^\gamma \bar{p}_t^\gamma \right) \\ &= 4(2q_t^\gamma - 1) dq_t^\gamma + 4(dq_t^\gamma)(dq_t^\gamma) + 4(dp_t^\gamma) \bar{p}_t^\gamma \\ &\quad + 4p_t^\gamma (d\bar{p}_t^\gamma) + 4(dp_t^\gamma)(d\bar{p}_t^\gamma) \\ &= 4(2q_t^\gamma - 1) \left([-ik_\gamma (p_t^\gamma - \bar{p}_t^\gamma) + \gamma \eta (1 - q_t^\gamma) q_t^\gamma] dt \right. \\ &\quad \left. - q_t^\gamma d\mathcal{N}_t^\gamma \right) \\ &\quad + 4(q_t^\gamma)^2 d\mathcal{N}_t^\gamma \\ &\quad + 4 \left([-ik_\gamma (2q_t^\gamma - 1) \bar{p}_t^\gamma + \gamma \left(-\frac{1}{2} + \eta - \eta q_t^\gamma \right) p_t^\gamma \bar{p}_t^\gamma] dt \right. \\ &\quad \left. - p_t^\gamma \bar{p}_t^\gamma d\mathcal{N}_t^\gamma \right) \\ &= \gamma (\eta - 1) 2(1 - q_t^\gamma) \left((r_t^\gamma)^2 + 2q_t^\gamma - 1 \right) \\ &\quad + (1 - (r_t^\gamma)^2) (\gamma (2q_t^\gamma - 1) dt + d\mathcal{N}_t^\gamma) . \end{aligned}$$

Appendix D: Convergence of spiking process for the scaling $k_\gamma \sim \gamma^\alpha$

We discuss the motivation behind the choice of $k_\gamma = \sqrt{\omega\gamma}$ in the Collapse-Unitary case in the main text. From numerical simulations (see Fig. 11), we determine that for the scaling $k_\gamma \sim \gamma^\alpha$, the distribution of the spiking process does not converge for large γ for $\alpha \gtrsim 0.5$ and the spikes vanish for large γ for $\alpha \lesssim 0.5$. This can also be seen by taking the limits $\omega \rightarrow 0$ and $\omega \rightarrow \infty$ in the first line of Eq. (25) (corresponding to $\alpha < 0.5$ and $\alpha > 0.5$ respectively). This provides credible justification for the form of k_γ that was assumed in the main text.

Appendix E: Exact computation and asymptotics of Laplace transforms

1. Collapse-Unitary setup

We derive the explicit expressions for the functions $C(\sigma)$, $D(\sigma)$ and $E(\sigma)$ (and their asymptotic forms for

large γ) to determine the generating function of the distribution of spikes for the Collapse-Unitary case. Thanks to the explicit expressions Eq. (35), we have then that

$$\begin{aligned} E(\sigma) &= \frac{1}{4(\beta')^2} \left\{ \frac{1 + e^{-2\phi}}{\sigma + \gamma/2 - 2\beta k_\gamma} \left(1 - e^{-(\sigma + \gamma/2 - 2\beta k_\gamma)\tau} \right) \right. \\ &\quad + \frac{1 + e^{2\phi}}{\sigma + \gamma/2 + 2\beta k_\gamma} \left(1 - e^{-(\sigma + \gamma/2 + 2\beta k_\gamma)\tau} \right) \\ &\quad \left. - \frac{4}{\sigma + \gamma/2} \left(1 - e^{-(\sigma + \gamma/2)\tau} \right) \right\} , \end{aligned} \tag{E1}$$

$$\begin{aligned} C(\sigma) + D(\sigma) &= \frac{\gamma}{4(\beta')^2} \left\{ \frac{e^{-2\phi}}{\sigma + \gamma/2 - 2\beta k_\gamma} \left(1 - e^{-(\sigma + \gamma/2 - 2\beta k_\gamma)\tau} \right) \right. \\ &\quad + \frac{e^{2\phi}}{\sigma + \gamma/2 + 2\beta k_\gamma} \left(1 - e^{-(\sigma + \gamma/2 + 2\beta k_\gamma)\tau} \right) \\ &\quad \left. - \frac{2}{\sigma + \gamma/2} \left(1 - e^{-(\sigma + \gamma/2)\tau} \right) \right\} , \end{aligned} \tag{E2}$$

and

$$\begin{aligned} D(\sigma) &= \left\{ \frac{e^{-2\phi}}{\sigma + \gamma/2 - 2\beta k_\gamma} \left(e^{-(\sigma + \gamma/2 - 2\beta k_\gamma)\tau_b} - e^{-(\sigma + \gamma/2 - 2\beta k_\gamma)\tau_a} \right) \right. \\ &\quad + \frac{e^{2\phi}}{\sigma + \gamma/2 + 2\beta k_\gamma} \left(e^{-(\sigma + \gamma/2 + 2\beta k_\gamma)\tau_b} - e^{-(\sigma + \gamma/2 + 2\beta k_\gamma)\tau_a} \right) \\ &\quad \left. - \frac{2}{\sigma + \gamma/2} \left(e^{-(\sigma + \gamma/2)\tau_b} - e^{-(\sigma + \gamma/2)\tau_a} \right) \right\} \times \frac{\gamma}{4(\beta')^2} . \end{aligned} \tag{E3}$$

We note the asymptotic forms for large γ (here we take $k_\gamma = \sqrt{\omega\gamma}$),

$$\begin{aligned} C(\sigma) &\sim 1 - (4\omega + \sigma) \gamma^{-1} - D(\sigma) , \\ D(\sigma) &\sim 4\omega \gamma^{-1} (\tan^2(b/2) - \tan^2(a/2)) , \\ E(\sigma) &\sim \gamma^{-1} . \end{aligned} \tag{E4}$$

Then Eq. (42) follows.

2. Collapse-Thermal setup

We derive the explicit expressions for the functions $C(\sigma)$, $D(\sigma)$ and $E(\sigma)$ (and their asymptotic forms for large γ) to determine the generating function of the distribution of spikes for the Collapse-Thermal case. Thanks to Eq. (50) we have that

$$\begin{aligned} E(\sigma) &= \frac{1}{q_+ - q_-} \left\{ \frac{q_+(1 - e^{-[\sigma + \eta\gamma(1 - q_-)]\tau})}{\sigma + \eta\gamma(1 - q_-)} - \frac{q_-(1 - e^{-[\sigma + \eta\gamma(1 - q_+)]\tau})}{\sigma + \eta\gamma(1 - q_+)} \right\} , \end{aligned} \tag{E5}$$

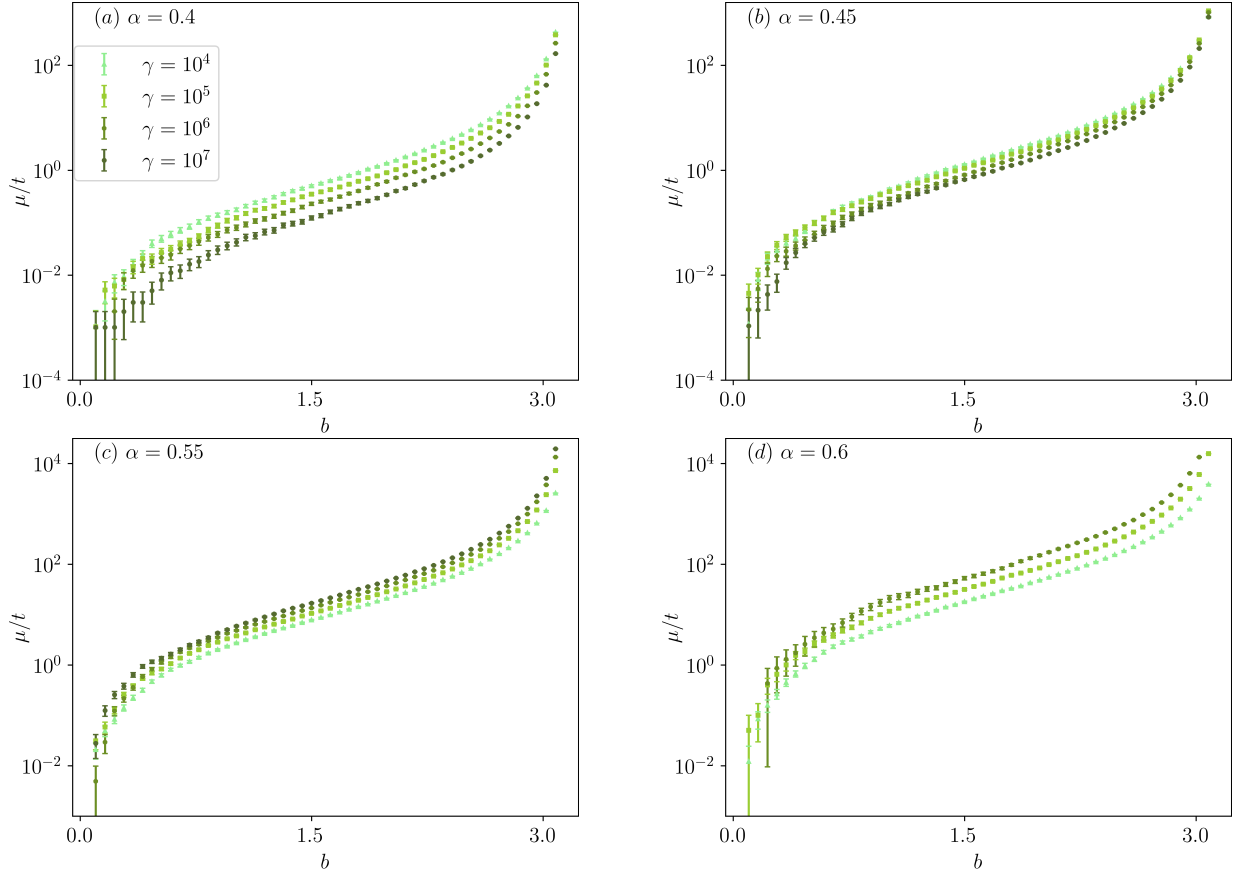


FIG. 11. Mean of the distribution (conditioned on no-jumps) of the number of spikes (from $\theta_t = \pi$) per unit time in a space-time box $(0, b) \times (0, t)$ plotted against the box edge b for (a) $k_\gamma \sim \gamma^{0.4}$ (b) $k_\gamma \sim \gamma^{0.45}$ (c) $k_\gamma \sim \gamma^{0.55}$ (d) $k_\gamma \sim \gamma^{0.6}$. The separation between the scatter plots for various γ is more than the width of the error bars and clearly indicates a downward trend with increasing γ for $\alpha = 0.4$ and $\alpha = 0.45$ (indicating that the spikes vanish for $\gamma \rightarrow \infty$) and clearly indicates an upward trend with increasing γ for $\alpha = 0.55$ and $\alpha = 0.6$ (indicating that the moments of the spike distribution diverge for $\gamma \rightarrow \infty$). The data-points were obtained by averaging over 10^4 realizations. Note that for $\alpha = 0.6$, we were not able to obtain data for $\gamma = 10^7$ since almost all the trajectories in the sample had the occurrence of jumps (recall that the spike distribution is conditioned on no-jumps).

We note then that the asymptotic forms of $E(\sigma)$, $C(\sigma)$ and $D(\sigma)$ for large γ are given by

$$C(\sigma) + D(\sigma) = \frac{\gamma\eta}{q_+ - q_-} \left\{ \frac{q_+(1-q_-)(1-e^{-[\sigma+\eta\gamma(1-q_-)]\tau})}{\sigma+\eta\gamma(1-q_-)} - \frac{q_-(1-q_+)(1-e^{-[\sigma+\eta\gamma(1-q_+)]\tau})}{\sigma+\eta\gamma(1-q_+)} \right\}, \quad (\text{E6})$$

$$E(\sigma) \sim \frac{1}{\sigma + \gamma\eta + W_{-,+}},$$

$$C(\sigma) \sim \frac{\gamma\eta - W_{-,+} \left(\frac{1}{a} - \frac{1}{b} \right)}{\sigma + \gamma\eta + W_{-,+}}, \quad (\text{E8})$$

$$D(\sigma) \sim \frac{W_{-,+} \left(\frac{1}{a} - \frac{1}{b} \right)}{\sigma + \gamma\eta + W_{-,+}}.$$

and

$$D(\sigma) = \frac{\gamma\eta}{q_+ - q_-} \left\{ \frac{q_+(1-q_-)(e^{-[\sigma+\eta\gamma(1-q_-)]\tau a} - e^{-[\sigma+\eta\gamma(1-q_-)]\tau b})}{\sigma+\eta\gamma(1-q_-)} - \frac{q_-(1-q_+)(e^{-[\sigma+\eta\gamma(1-q_+)]\tau a} - e^{-[\sigma+\eta\gamma(1-q_+)]\tau b})}{\sigma+\eta\gamma(1-q_+)} \right\}. \quad (\text{E7})$$

Then Eq. (51) follows.

3. Collapse-Measurement setup

We derive the explicit expressions for the functions $C(\sigma)$, $D(\sigma)$ and $E(\sigma)$ (and their asymptotic forms for

large γ) to determine the generating function of the distribution of spikes for the Collapse-Measurement case. Thanks to Eq. (59) we have that

$$E(\sigma) = \frac{1}{\gamma_1\eta_1 + \gamma_2} \left\{ \frac{\gamma_2(1-\eta_2)(1-e^{-\sigma\tau})}{\sigma} + \frac{(\gamma_1\eta_1 + \gamma_2\eta_2)(1-e^{-(\sigma+\gamma_2+\gamma_1\eta_1)\tau})}{\sigma+\gamma_2+\gamma_1\eta_1} \right\}, \quad (\text{E9})$$

$$C(\sigma) + D(\sigma) = \frac{\gamma_1\eta_1(1 - e^{-(\sigma+\gamma_2+\gamma_1\eta_1)\tau})}{\sigma + \gamma_1\eta_1 + \gamma_2}, \quad (\text{E10})$$

and

$$D(\sigma) = \frac{\gamma_1\eta_1(e^{-(\sigma+\gamma_1\eta_1+\gamma_2)\tau_a} - e^{-(\sigma+\gamma_1\eta_1+\gamma_2)\tau_b})}{\sigma + \gamma_1\eta_1 + \gamma_2}. \quad (\text{E11})$$

We note then that the asymptotic forms of $E(\sigma), C(\sigma)$ and $D(\sigma)$ for large γ_1 are given by

$$\begin{aligned} E(\sigma) &\sim \frac{1 - \frac{\epsilon\gamma_2(1-\eta_2)}{\sigma+\gamma_1\eta_1+\gamma_2}}{\sigma + \gamma_1\eta_1 + \gamma_2}, \\ C(\sigma) &\sim \frac{\gamma_1\eta_1 - \gamma_2(1-\eta_2)\left(\epsilon + \frac{1}{a} - \frac{1}{b}\right)}{\sigma + \gamma_1\eta_1 + \gamma_2}, \\ D(\sigma) &\sim \frac{\gamma_2(1-\eta_2)\left(\frac{1}{a} - \frac{1}{b}\right)}{\sigma + \gamma_1\eta_1 + \gamma_2}. \end{aligned} \quad (\text{E12})$$

Then Eq. (60) follows by taking the limit $\gamma_1 \rightarrow \infty$.

Appendix F: Numerical Methods

Here, we discuss the two numerical methods employed to simulate the 1D stochastic differential equations (SDEs) with Poissonian noise that govern the evolution of the state x_t . The first method is a first-order iterative approach where, given an SDE with Poissonian noise:

$$\begin{aligned} dx_t &= f(x_t)dt + h(x_t)dN_t, \\ dN_t dN_t &= dN_t, \\ \mathbb{E}[dN_t] &= g(x_t)dt, \end{aligned} \quad (\text{F1})$$

$\{x_t\}_{t=\Delta t, 2\Delta t, \dots}$ is obtained using the rule

$$x_{t+\Delta t} = x_t + f(x_t)\Delta t + h(x_t)r_t, \quad (\text{F2})$$

where the step-size $\Delta t \ll 1$ is chosen appropriately and the random number r_t is sampled from a Bernoulli distribution with the parameter $p = g(x_t)\Delta t$.

The second method is based on the principle that the stochastic evolution Eq. (F1) is composed of deterministic flows and jumps (not to be confused with quantum jumps). Discarding the Poissonian noise, Eq. (F1) becomes a first order ODE: $\dot{x}_t = f(x_t)$ which, given the initial condition $x_{t=0} = x_0$, has the unique solution x_{t,x_0} . Now, the probability $\nu(t, x_0)$ of having no-jumps in an interval $(0, t)$ with the initial condition $x_{t=0} = x_0$ is formally given by:

$$\nu(t, x_0) = \exp\left(-\int_{x_0}^{x_{t,x_0}} \frac{g(x)dx}{f(x)}\right), \quad (\text{F3})$$

We now have all the ingredients necessary for this method. Given that the state at time t_i is x_{t_i} , the algorithm for time evolution is as follows:

1. Choose a random number τ from the distribution $-\frac{\partial\nu(t, x_{t_i})}{\partial t}$, where $\nu(t, x_{t_i})$ is given by Eq. (F3). Physically speaking, this means that a jump has occurred at time $t_{i+1} = t_i + \tau$ and from the deterministic flow, we know the state takes the values $x_{t'} = x_{t'-t_i, x_{t_i}}$ for $t_i \leq t' < t_{i+1}$.
2. The value of the state at time t_{i+1} is set by $x_{t_{i+1}} = h(x_{\tau, x_{t_i}})$.
3. Repeat steps 1 & 2 with the transformations $t_i \rightarrow t_{i+1}$ and $t_{i+1} \rightarrow t_{i+2}$.